

# 2021 NIAC Phase I Final Report

Extrasolar Object Interceptor and Sample  
Return Enabled by Compact, Ultra Power  
Dense Radioisotope Batteries

PI: Christopher Morrison Ph.D.

## Table of Contents

<b>TABLE OF CONTENTS</b>	<b>II</b>
<b>QUAD CHART</b>	<b>III</b>
<b>EXECUTIVE SUMMARY</b>	<b>IV</b>
<b>1. MISSION CONTEXT – EXTRASOLAR OBJECT SAMPLE RETURN MISSION</b>	<b>1</b>
SCOPING CALCULATION	2
TRAJECTORY ANALYSIS WITH METHOD OF PATCHED CONICS	2
‘OUMUAMUA RENDEZVOUS MISSION	6
MISSIONS TO THE OUTER PLANETS	7
MISSION COMPATIBILITY WITH OTHER TECHNOLOGIES	7
<b>2. RADIOISOTOPE POWER SYSTEMS BACKGROUND</b>	<b>7</b>
HISTORY	7
THEORETICAL ENERGY	8
GENERIC RADIOISOTOPE PRODUCTION	11
<b>3. ENABLING TECHNOLOGY – EMBERCORE™</b>	<b>13</b>
ENCAPSULATION SAFETY	14
EMBER FABRICATION	14
CRITERA FOR PRE-ACTIVATION ENCAPSULTION AND CHARGING OF RADIOISOTOPE	16
ISOTOPE SELECTION AND TARGET DESIGN FOR CO-60	18
X-RAY AND GAMMA-RAY SHIELDING	21
SUPPLY CHAIN AND PRODUCTION	23
EMBERCORE COMMERCIAL PRODUCT FOR LUNAR MARKET	25
<b>4. REGULATORY AND LAUNCH SAFETY</b>	<b>27</b>
GROUND LICENSING	27
SPACE LICENSING	28
REGULATORY QUALIFICATION MISSION	30
<b>5. EXTRASOLAR EXPRESS SPACECRAFT</b>	<b>32</b>
SPACECRAFT SUBSYSTEMS	36
High Temperature Power Conversion	37
Electric Propulsion	38
Thermal Management	39
Structure	41
Radiation Dose Management	43
Sample Return Payload	45
MISSION CONOPS	45
<b>6. PHASE II AND PHASE III TECHNOLOGY MATURATION PLAN</b>	<b>45</b>
<b>7. CONCLUSION</b>	<b>47</b>
<b>8. ACKNOWLEDGEMENTS</b>	<b>49</b>
<b>9. REFERENCES</b>	<b>50</b>

# Extrasolar Object Sample Return Mission: Enabled by EmberCore an Ultra Power-Dense Radioisotope Technology

Dr. Christopher Morrison/USNC-Tech

## Innovation

- Radioisotope electric propulsion for sample return from an extrasolar object - start to finish 10 years
- Co-60 EmberCore radioisotope, up to 30x thermal power density of Pu-238, easy to manufacture in existing facilities, strong launch safety case
- High temp. solid-state power conv.  $< 5 \text{ kg/kW}_e$
- Spacecraft design for radioisotope
- $\Delta V$  capability  $\sim 100 \text{ km/s}$
- Compact & scalable

## Technical Approach

- (50%) Target Design
  - Ember Prototypes
  - Regulatory
  - Supply Chain
- (15%) Trajectory
- (35%) Power Conversion & Vehicle Design



## Benefits

- Easy to manufacture radioisotope from available facilities with common materials (Cobalt) in reasonable time periods (6 months – 1 year)
- Strong radioisotope safety case based on proprietary encapsulation methods and aeroshell
- First science on an extrasolar object!
- Small simple system (1.2 ton wet mass, 200 kg dry mass) with  $\sim 5 \text{ kg/kW}_e$  power system

## Phase I Results

- Raising TRL of EmberCore is straightforward
- Multiple power conversion options, some higher TRL
- A 100 km/s mission enables sample return on a 10-year timeline
- A 2030 flight of the Extrasolar Express is credible
- Key challenge to flight is regulatory/launch approval, not technological

## Executive Summary

Before 2017 extrasolar objects, such as 'Oumuamua, were unknown. Mission architectures well-suited to extrasolar object study were not envisioned. Extrasolar objects are somewhat unique in their trajectory, as they fall into the sun's gravity well, they gain incredible speeds, however they are not incredibly far away and often fall into the inner solar system. To catch an extrasolar object, you don't need to be a marathon runner, but instead you must be a sprinter. This was a key insight for this NIAC. Short-lived but high-power density radioisotopes were recognized as a "sprinter" architecture which could catch the extrasolar objects as they come into the solar system sample the object, and finally come back to Earth before the object travel an extreme distance. While NASA had looked at these types of isotopes in the past, they were ultimately rejected in favor of Pu-238 a longer lived, lower power density radioisotope (more of a marathon architecture).

Radioisotopes have challenges associated with them. Among those challenges are the cost and supply of radioisotopes, the regulatory restrictions on the nuclear materials, the x-rays emitted from the material that can damage human and computer systems. Traditional radioisotopes require significant radiochemical processing which involves a facility which takes a material dissolves it in acid, concentrates isotopes of interest, and goes through many steps before the final material is produced. This process has many commonalities with Plutonium-239 weapons production and is highly regulated.

However, that is where the key technical innovation behind this NIAC comes in. USNC-Tech has developed a patent pending method for production of radioisotopes which eliminates the need for radiochemistry, doesn't use any exotic materials, has a large degree of inherent safety, and finally can produce several different useful radioisotopes. The production method involves manufacturing an encapsulated composite ceramic pellet called an "ember" in a non-rad facility, irradiating the pellet in a fission reactor which activate the encapsulated nuclear ceramic, and then finally installing the pellets into an EmberCore™. This modular radioisotope production architecture eliminates many of the key challenges related to traditional radioisotopes and greatly reduces the cost and enables production. In fact, recently USNC-Tech produced the first small quantity of Tm-170 radioisotope at the Reed Research Reactor and has a pathway for production of kW-scale quantities over the next three years.

USNC-Tech is currently developing a 1-40 W EmberCore heater focused on enabling lunar night survival for commercial and NASA payloads on the lunar surface looking at a 2024 demonstration. The EmberCore proposed for this NIAC utilizes the same technology architecture as the lunar heater but is higher power and higher temperature and utilizes high temperature power conversion to generate electricity.

Building off the legacy of the NASA's MMRTG, EmberCore is designed with launch safety and regulatory licensing in mind. A defense in depth approach is utilized which involves multiple redundant engineered layers designed to hand launch failure including re-entry, impact, fire, and combinations thereof.

A key development for the EmberCore technology was the release of the 2019 National Security Presidential Memorandum 20. The memo establishes for the first time a pathway for a commercial company to obtain launch approval through a tiered system with clearly defined risk and material-based criteria. USNC-Tech engaged in with the FAA and the NRC and significant amounts for effort in the Phase I NIAC were spent evaluating both space and ground handling regulatory requirements.

The radioisotope electric propulsion spacecraft concept, dubbed the “Extrasolar Express,” designed during this Phase I NIAC is capable of a  $\Delta V$  of 100 km/s and has several key innovations.

One innovation is utilizing an ejectable shield. On the ground and during launch, a heavy shield is included to protect ground crews. However, once in a safe orbit, the heavy shield and aeroshell are ejected making the spacecraft low mass.

The vehicle takes advantage of the high temperature capability of the refractory EmberCore technology. The power conversion system utilizes high temperature solid state power conversion (thermoelectric and thermionic technologies were evaluated) providing a power subsystem specific power of 5 kg/kW<sub>e</sub> – which enables fast sample return missions. This Phase I NIAC utilized the GMAT astrodynamics tools to demonstrate the return Extrasolar Object sample return capability by modeling a hypothetical mission to ‘Oumuamua with a launch date the day that ‘Oumuamua was discovered.

While there are other technologies that can achieve the low specific mass (such as fission), a unique feature of the EmberCore technology is its ability to scale down to a small size and launch mass. The 10 kW<sub>e</sub>, 100 kW<sub>th</sub> beginning of life baseline spacecraft design with a 20 kg payload has a wet mass of 1200 kg. Including the 3 metric ton ejectable shield, the launch mass of the spacecraft was a little over 4 metric tons which fit in small launch vehicles. Assuming the payload mass is proportionally reduced, the spacecraft power can be further miniaturized and still obtain 100 km/s capability.

In contrast to a radioisotope, a fission power system cannot be scaled down as the reactor core requires a critical mass. A comparable 5 kg/kW<sub>e</sub> power system would require a mass around two orders of magnitude greater.

The main isotope of interest for this project is Co-60. It is easy to produce as an ember, has a half-life of 5.27 years (which is very compatible for the extrasolar missions), and has an extremely high-power density. One key drawback is that it is strong gamma emitter which complicates ground crew handling and can damage electrical components. The ejectable shield is more than enough to protect the ground crew however once the shield is ejected, the payload, power modulation, and other sensitive components need to be protected.

Several strategies were chosen to reduce the dose to sensitive components. A small, depleted uranium shadow shield and spot shielding were employed to provide mass effective shielding. A deployable boom was considered to increase the distance from the radioactive source, and rad hardened components with a 100 - 1000 krad dose tolerance were considered. However, a key development during the design process was the selection of liquid metal FEEP thrusters. Liquid Indium was used for the FEEP thruster propellant. The density of the propellant made it an excellent shielding material. In addition, the Indium metal has a low vapor pressure which allows for tanks to be designed in non-spherical shapes. These shapes are designed in long tubes which provided superior radiation shielding.

The solid-state power conversion system is also resilient against x-ray radiation. Heat pipe performance is unaffected by x-ray radiation and thermionic and to a lesser extent thermoelectric power conversion technology is highly resilient against x-ray radiation. In some cases (bearing future experimental support) intense x-rays improve the performance of these power conversion devices by increase the electrical conductivity. A conclusion of the Phase I study suggests that the power conversion system does not need to be shielded.



## 1. Mission Context – Extrasolar Object Sample Return Mission

In the past four years, we have detected the first two known interstellar objects passing through our solar system: Oumuamua in 2017 and C/2019 Q4 (Borisov) in 2019. Both interstellar objects contain a wealth of undiscovered information about what the universe is like outside our solar system. Being able to visit, take a sample from these extrasolar objects, and return them to Earth for study has the potential to fundamentally change our view of the universe and its evolution.

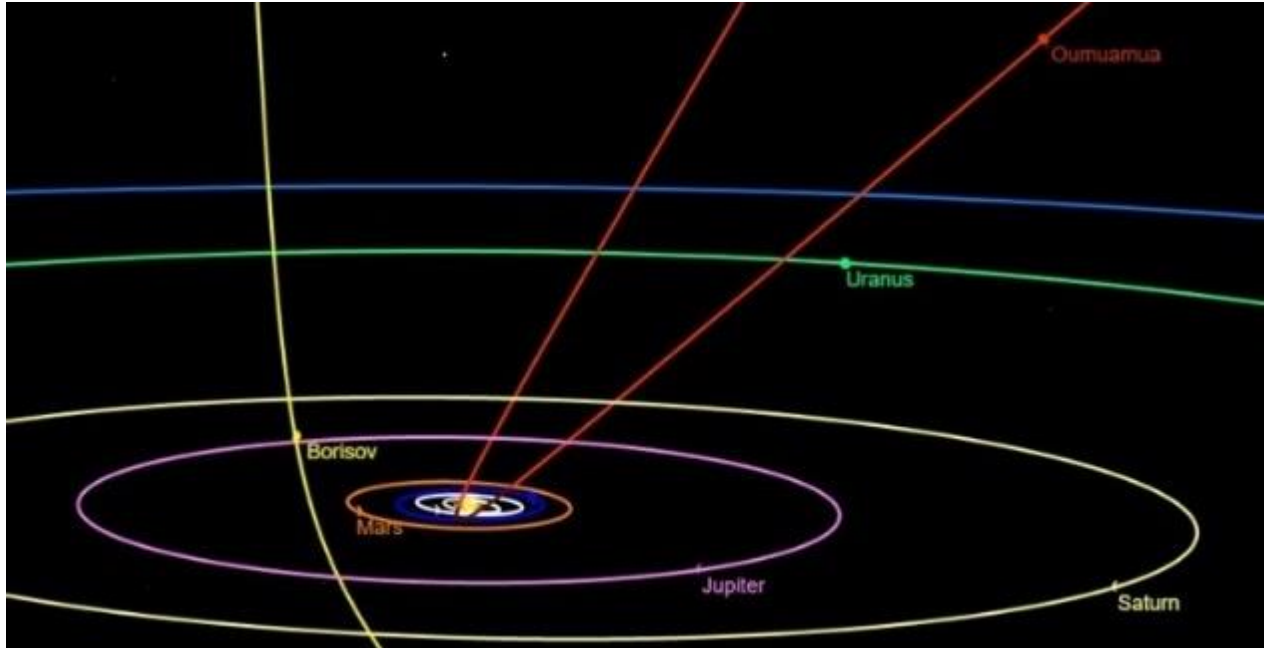


Figure 1: Trajectories of interstellar objects 'Oumuamua and C/2019 Q4 (Borisov) shown in red and yellow respectively <sup>1</sup>.

	Segment		km/s	Notes
Rendezvous	1	$\Delta V_{earth,escape}$	$> 3.3$	For low thrust electric propulsion can be as high as 6.6 km/s
	2	$\Delta V_{solar.escape}$	$> 12.3$ $< \sim 42$	Escaping the solar system requires 42 km/s at 1 AU. Earth can provide about 30 km/s depending on how well a positioned the extrasolar object is and how well a plane change could be executed.
	3	$\Delta V_{\infty}$	10 to $> 30$	Depends on the extrasolar object velocity.
	4	$\Delta V_{fast}$	10 to $> 30$	Speed up to close the distance between the object and slow down for rendezvous. Highly dependent upon the distance of the extrasolar object's intersection with the solar plane from Earth and how early the object was spotted.
Return	5	$\Delta V_{\infty}$	10 to $> 30$	Depends on the extrasolar object velocity.
	6	$\Delta V_{solar.dive}$	$> \sim 5$ $< \sim 12.3$	Required to bring orbit to Earth intercept. Possible to use other plants as a gravity assist or possibly an aerobrake.
		<b>Total</b>	<b>50.6 – 148</b>	This wide range of required $\Delta V$ serves as a simple first order bound.

Table 1: First Order Delta-V Mission Requirements Estimates

## Scoping Calculation

With the completion of the Large Synoptic Survey Telescope (LSST) in 2022<sup>2</sup>, the expected detection rate for interstellar objects is expected to increase from 0.2/y to 1/y<sup>3</sup>. If this expectation is correct, there will be many opportunities to study and visit an interstellar object. However, a spacecraft must first exist to perform the mission. Shortly before the appearance of C/2019 Q4 (Borisov), the first interstellar comet interceptor mission was approved through the ESA's Cosmic Vision Programme<sup>4</sup>. However, this mission cannot rendezvous with an interstellar object and return, it can only perform a flyby. This is because of the extremely high velocities of these objects as they pass through the solar system. 'Oumuamua was recorded at a velocity of 26.33 km/s as it entered the solar system<sup>5</sup> while C/2019 Q4 (Borisov) has been measured at 32.6 km/s as it entered the solar system<sup>6</sup> relative to the Sun (this velocity is also known as  $V_{\infty}$ ). The  $\Delta V$  required to perform the sample return can be roughly estimated. Assuming a starting orbit in LEO, **Table 1** **Error! Reference source not found.** goes into the basic details of what an extrasolar object intercept and sample return mission would require.

For the purposes of this proposal, 100 km/s is assumed to be a reasonable value but could be as little as 50 or greater than 150 km/s based upon the trajectory of the object, the amount of time the object was detected before it makes the closest approach to Earth, the speed at which the mission is desired to be carried out and finally any favorable planetary alignments that may allow for gravity assists. Chemical propulsion cannot feasibly achieve a  $\Delta V$  exceeding 20 km/s. Electric propulsion can achieve  $\Delta V$  on the order of 100 km/s but requires a power source that can operate at vast distances from the sun and with a low mass. The specific mass required for this mission can be estimated on the first order.

$$\Delta V = I_{sp} g_o \ln \left( \frac{m_o}{m_o - m_{prop}} \right) \quad \text{Eq. 1}$$

$$P = E/t = m_{prop} \frac{(I_{sp} g_o)^2}{2 t \eta_{thruster}} \quad \text{Eq. 2}$$

The findings in Table 2 below show that an  $I_{sp}$  around 8200 s allows for the easiest requirements for the power source specific mass.

Table 2: Optimal  $I_{sp}$  given Mission Assumptions

$I_{sp}$ [s]	Prop. Frac.	t = 5 years	t = 10 years	t = 15 years	Assumptions	
		Power Source Specific Mass [ kg/kW <sub>e</sub> ]			Tank Mass	10%
4000	0.941	2.798	7.597	12.395	$\eta_{thruster}$	65%
6000	0.849	6.814	15.629	24.443	Payload Mass	2.5%
8000	0.757	7.569	17.139	26.708	$\Delta V$	100 km/s
8200	0.749	7.573	17.146	26.718	Thruster Alpha	2 kg/kW <sub>e</sub>
9000	0.716	7.517	17.033	26.550	Jettison Tanks	

From Table 2 the power source specific mass requirements for the 8200 s  $I_{sp}$  case can be seen. For a five-year, ten-year, and fifteen-year-round trips specific masses of 7.5, 17.14 and 26.7 kg/kW<sub>e</sub> respectively are required.

## Trajectory Analysis with Method of Patched Conics

The goal of this mission is to intercept Oumuamua and then return to Earth in the shortest possible time, given that the spacecraft launches on October 18, 2017, the day that Oumuamua was discovered. The

spacecraft described in this report uses a thruster that fires continuously with a total  $\Delta V$  budget of 100 km/s over several decades.

Though the spacecraft being investigated fires its thruster continuously, the problem is simplified by assuming that all thrust is instantaneous and occurs at singular moments during the execution of the mission. This simplification allows the mission to be approximated by the patched conics method used for preliminary mission design. The patched conic solver Optimum Interplanetary Trajectory Software (OITS) created by Dr. Adam Hibberd was employed for this calculation.

A number of mission configurations were considered to reach Oumuamua, including the following:

- Earth – Deep Space Maneuver – Earth – Jupiter – Oumuamua
- Earth – Deep Space Maneuver – Earth – Jupiter – Saturn – Oumuamua
- Earth – Deep Space Maneuver – Earth – Jupiter – Sun Oumuamua

Many of these mission configurations were investigated due to the promise they indicated in other investigations [LINK]. However, the objectives of the missions tested in these other papers do not align with those in this paper. Ordinarily, the challenge of interplanetary mission design lies in finding a way to exploit the motion of other celestial bodies to supplement a very finite supply of fuel, and consequently  $\Delta V$ , in order find the most efficient path to a target. However, the  $\Delta V$  budget of the spacecraft proposed in this paper far exceeds those of other modern spacecraft and of those investigated in other papers concerning missions to Oumuamua. Consequently, the objective of the mission described in this paper is not to be efficient but is instead to best capitalize on the abundance of  $\Delta V$  that this thruster affords to intercept Oumuamua and return to Earth in the minimum amount of time. Since this spacecraft has a  $\Delta V$  budget necessary to execute costly and ordinarily infeasible plane change maneuvers, the selected mission profile opts to eschew time-consuming journeys to other bodies for gravity assists, and instead uses its  $\Delta V$  budget to transfer almost directly to Oumuamua before returning directly to Earth. Notably, since the actual spacecraft fires its thruster continuously instead of in high-impulse instantaneous bursts, plane-change gravity assists that pass close to the sun or other bodies are avoided, since they require great instantaneous acceleration at specific points around their central bodies.

The optimal mission profile found in this investigation is the following:

- Earth Launch – Deep Space Maneuver – Oumuamua – Earth Return

Using the patched conic method, it is implied that thrust is being applied instantaneously at each of these four locations, though in actuality, the velocity required at each of these points is accumulated by firing the thrusters over extended periods of time.



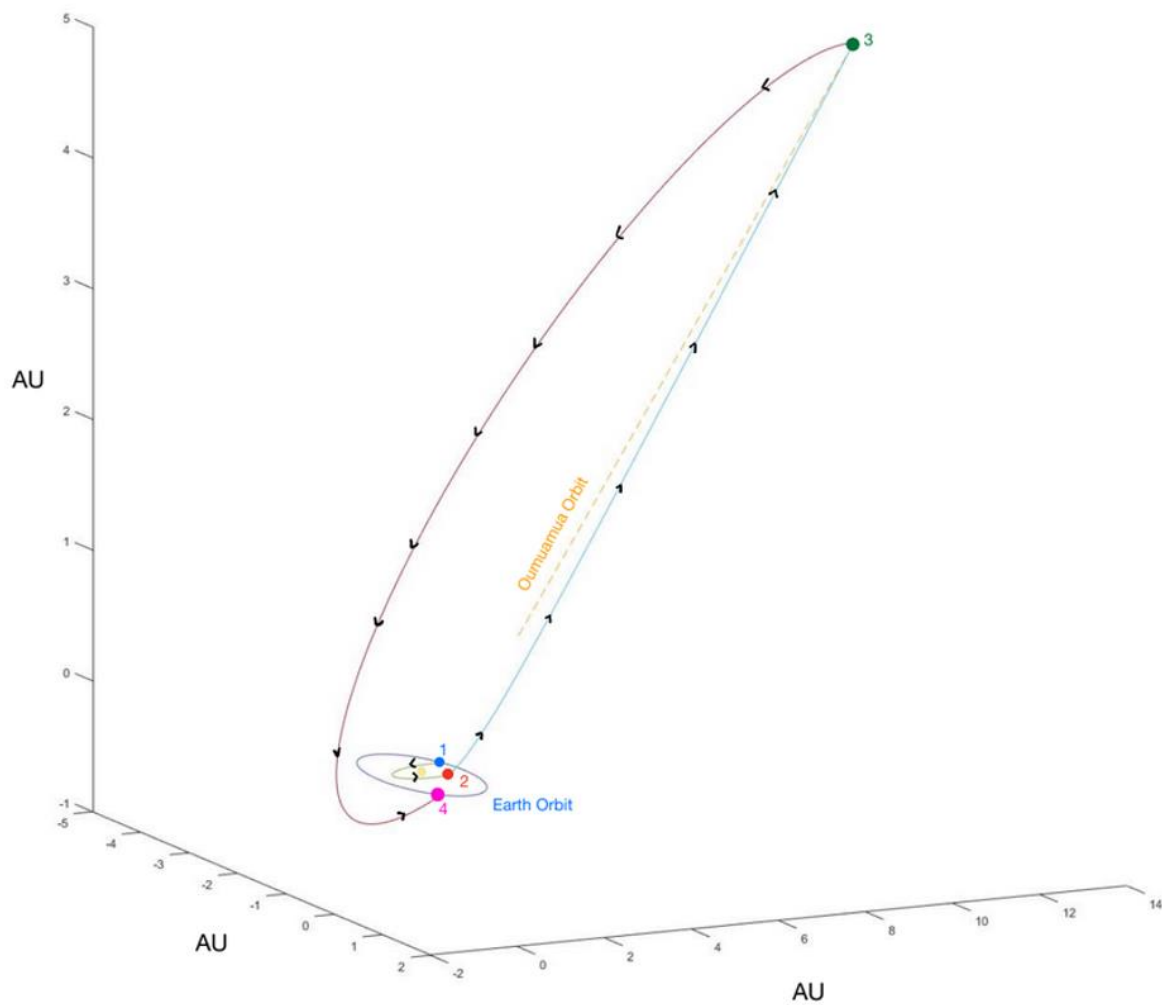


Figure 2: Mission Profile Plot

Table 3: Mission Profile Timeline

	Title	Time	DeltaV (km/s)	Cumulative DeltaV (km/s)
1	Earth Departure	2017 OCT 15	9.63	9.63
2	Plane Change	2018 FEB 01	27.78	37.41
3	Oumuamua Arrival	2019 SEP 06	36.3	73.71
4	Earth Arrival	2030 MAY 21	23.14	96.85

Figure 2 depicts the plot of the most optimal mission profile found in this investigation while *Table 1* describes the  $\Delta V$  expended at each point in the mission. This mission, launching on Oumuamua's discovery date, takes a mere 23 months to intercept Oumuamua, and then another eleven years to return to Earth.

The first leg of mission, starting at point 1, departs from Earth and drops the spacecraft into an elliptical orbit around the Sun. This serves to reorient the motion of the spacecraft. At the time of launch, the velocity vector of the Earth and of the spacecraft is out of alignment with the motion of Oumuamua. This is most obvious if viewed from the top-down orthographic view in Figure 3.

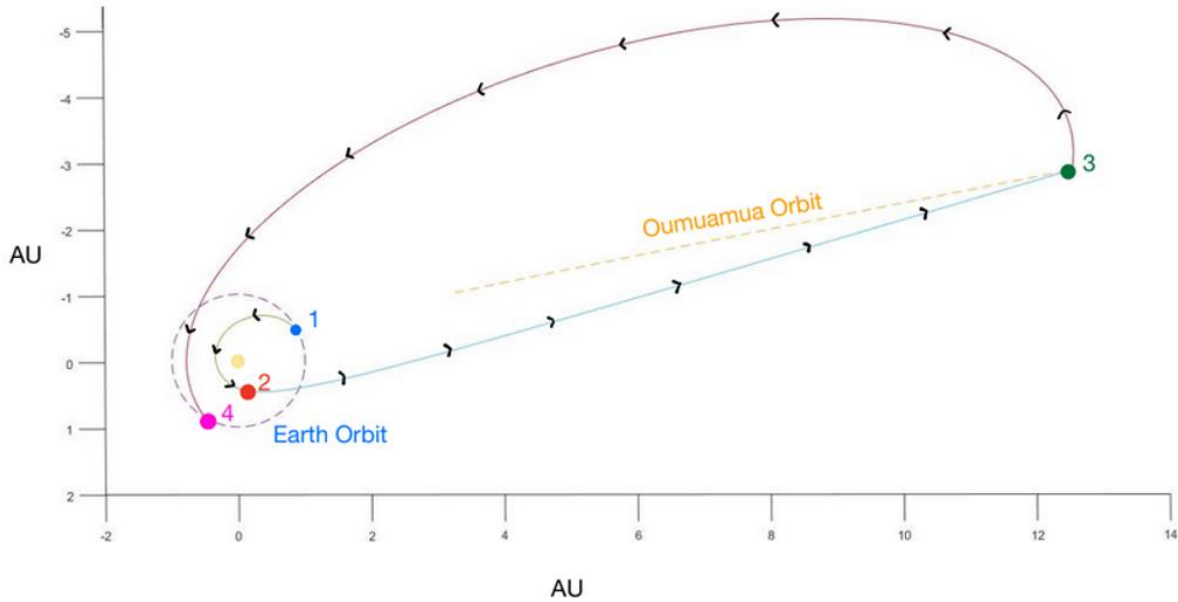


Figure 3: Top Down Orthographic View

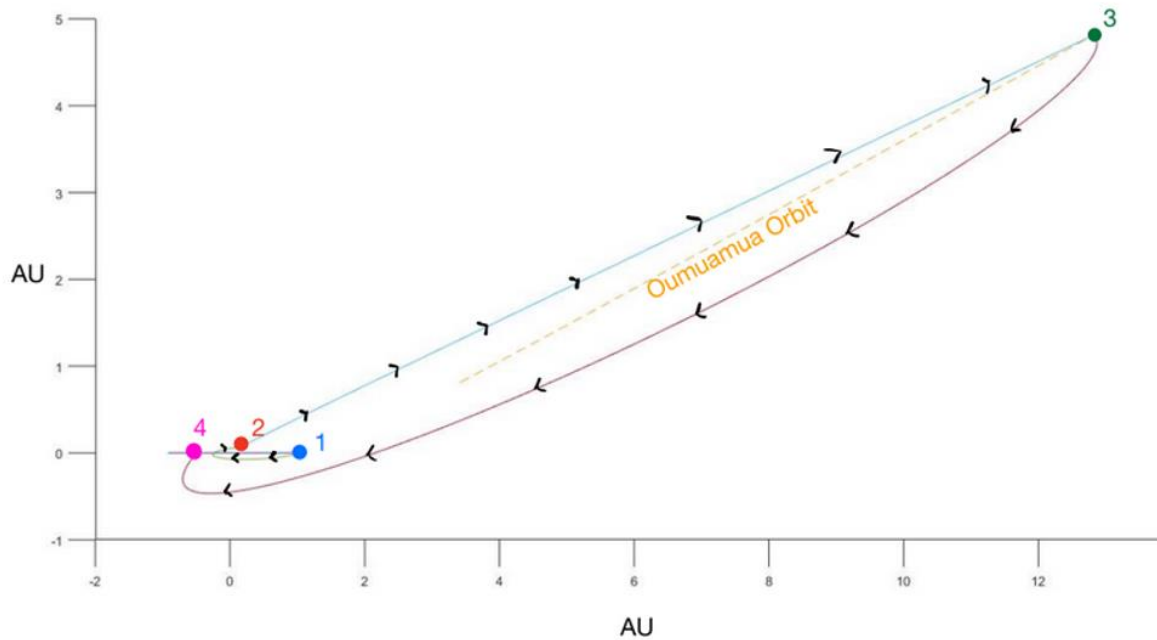


Figure 4: Side Orthographic View

At Point 1, Oumuamua is already traveling away from the sun and out of the Solar System. By dropping the spacecraft into an elliptical orbit around the Sun, the spacecraft's velocity vector will be facing the path of Oumuamua's travel by the time it reaches Point 2.

Point 2 marks the second leg of the mission, wherein the spacecraft must boost into a hyperbolic orbit with respect to the Sun and change the plane of its orbit to intercept Oumuamua. Not only does the spacecraft need to propel itself to catch up to Oumuamua as seen in *Figure 2*, but it also needs to enter an orbital plane inclined from the plane of Earth's orbit, seen in *Figure 3*.

Again, it is crucial to remember that the  $\Delta V$  expended at Point 2 is expended over time, and that this plane change will take place gradually over the course of the second leg of the mission.

Point 3 marks the spacecraft's arrival at Oumuamua, and the beginning of the return to Earth. At this point, the spacecraft will reorient its thruster to drop from its hyperbolic heliocentric orbit and return to an elliptical orbit with respect to the Sun. The  $\Delta V$  required to perform this maneuver is high since at this point the spacecraft must counteract the momentum of its path to Oumuamua and change the direction of its velocity vector to match that of its new elliptical path.

Midway through this final leg of the journey, the spacecraft will begin to burn to lower the energy of its orbit to have zero velocity with respect to the Earth at the time of its arrival. This is represented by the  $\Delta V$  expenditure occurring at Earth Arrival in *Table 1*.

This is a preliminary investigation into the sorts of missions that would be made possible by this technology. As such, there are several ways in which this analysis could be refined in the future.

The most obvious refinement would be to model the thrust of the spacecraft as a continuously burning thruster, rather than as one that fires instantaneously. Though this makes optimization more difficult, it would make mission profile more accurate to the behavior of the actual spacecraft. This is the most significant improvement that could be made to this mission analysis. Furthermore, the patched conic method employed in this solution does not account for the perturbations caused by bodies not immediately involved with each encounter. These perturbations would need to be accounted for in the final analysis. A Phase II investigation will address these limitations with a higher fidelity simulation and more mission scenarios.

## 'Oumuamua Rendezvous Mission

The 'Oumuamua extrasolar object has been a subject of great interest and contention to astronomers. While traveling on close approach to the sun the object displayed a change in velocity that could not be explained by gravity alone. In addition, the shape of the object was peculiar. The object had a large aspect ratio initially believe to be "cigar" shaped, but later to be disk shaped. This shape is odd because such an object traveling through interstellar space over a long period is subject to erosion by cosmic rays and should have broken apart.<sup>10, 11</sup>

Initially scientists were operating under the theory that there is nothing special about 'Oumuamua. The acceleration could be explained by outgassing of a frozen volatile like a comet. The lack of detectable tail ruled out many volatiles and nitrogen gas volatiles have been proposed. However, many in the scientific community believe that a nitrogen ice formation without additional detectable gasses would be rare. Regardless of the proposed natural or non-natural origin stories for 'Oumuamua it is an unprecedented object for study, and it is unknown if an object like it will be seen again.<sup>12,13</sup>

An 'Oumuamua rendezvous represents a tantalizing additional attractive mission architecture and has been studied in a series of papers under the codename Project Lyra<sup>14</sup> by the Initiative for Interstellar Studies. Based on their studies a  $\Delta V$  on the order of 35 km/s combined with some gravity assists would enable a flyby of 'Oumuamua within 15 years if the mission was launched by the late 2020s. A higher  $\Delta V$  on the order of 50 – 100 km/s would easily enable a much faster flyby, a rendezvous mission, or possibly a sample return mission given enough time to account for the distance that 'Oumuamua has travelled (on the order of 80-150 AU depending on mission context).

## Missions to the Outer Planets

Based on feedback during this Phase I NIAC, many scientists we talked with were quick to point out the benefits to a mission to the outer planets, especially Uranus and Neptune. While lower performance MMRTG based radioisotope electric propulsion missions have been proposed, the travel time can be a decade or more. A high specific mass and  $\Delta V$  mission to these locations would greatly reduce the mission time and would enable a more aggressive exploration (active propulsion for fast transit to different locations of interest such as moons and deeper gravity wells).

## Mission Compatibility with Other Technologies

Advanced solar power sources at 1 AU can obtain a specific mass around 10 kg/kW<sub>e</sub><sup>6</sup>, however given the long distances from the sun involved, solar electric propulsion is not feasible. Pu-238 MMRTGs are low power density achieves a specific mass close to 400 kg/kW<sub>e</sub><sup>7</sup> far short of the 7.5-26.7 kg/kW<sub>e</sub> needed. TRL 2/3 fission power systems have been proposed which can reach the specific mass goals, however fission systems require a minimum critical mass.

Fission can achieve the specific mass performance needed, but a drawback is the mass requires a critical mass to instantiate a fission reaction requires a large spacecraft with 50 to 100 tons dry mass and 200 to 1000 metric tons of wet mass.<sup>8</sup> A fission system a system would require significant launch efforts and require on orbit assembly which would not be amenable to a quick response to transitory extrasolar objects. Radioisotopes on the other hand are smaller and nimbler for exploration.

Sunjammer solar sails, which fly within a few solar radii of the sun, can also achieve a high  $\Delta V$  approaching that of 100 km/s<sup>9</sup> and have been the subject of recent NIAC studies. However, the challenge with solar sail technology is that once far from the sun, those architectures cannot slow for rendezvous or return to Earth. Sunjammer-like solar sails could theoretically be paired with a radioisotope power system to increase the performance. Such an architecture though would need to be fleshed out as the low area mass sail and high-density radioisotope would need to be mechanically coupled.

## 2. Radioisotope Power Systems Background

### History

Radioisotopes for power production are a well-known and proven technology. Radioisotope thermal generators have been used for nearly 60 years. The U.S. over 30 units for space operations including the Apollo mission. NASA originally utilized many different radioisotopes including Ce-144, Po-210, Sr-90. In the 1960's -1980's low power pacemakers were developed using Pu-238 and Pm-147. However, today NASA only utilizes the Pu-238 technology.

The Russians were able to mass produce Sr-90 by processing their nuclear fuel. The Soviets were able to solve the supply challenges and deployed over 1500 nuclear batteries throughout the world. However, the Sr-90 power units faced safety challenges. There have been multiple cases of significant radioactive material release from dilapidated and damaged units. Today these power units are a safety liability and are not under consideration as a commercial technology. The lesson to be learned from the Soviets is that, without a robust method of encapsulating and isolating nuclear material from environmental release, commercialization of nuclear battery technology is not feasible.

To be successful radioisotope technology must be able to achieve the following.

1. **Safety:** can the technology be shown to be safe under all credible circumstances?
2. **Technical/Manufacturing:** technology development and manufacturing be proven?
3. **Regulatory:** are the regulatory frameworks established and complied with?
4. **Market:** is the technology able to compete on performance and attract customers?

Generally, radioisotope technology for power production has had only limited success, however radioisotope production for medicine and industrial use is very much the opposite story. In fact, in the early days of atomic physics, experimentalists such as Marie Curie would obtain their radioactive sources from hospitals which typically carried Radium for cancer treatment. In 2020 the global medical radioisotope market is valued at 15 billion dollars. While much of this market is focused on diagnosis there are a few medical (and industrial) radioisotopes which produce large quantiles of power. Specifically, Cobat-60 is produced in the medical industry in quantities on the order of 100 kW of thermal power each year.

### Theoretical Energy

Radioisotopes contain on the order of one million times the energy density of state-of-the-art chemical batteries and fossil fuels as shown in Figure 5.



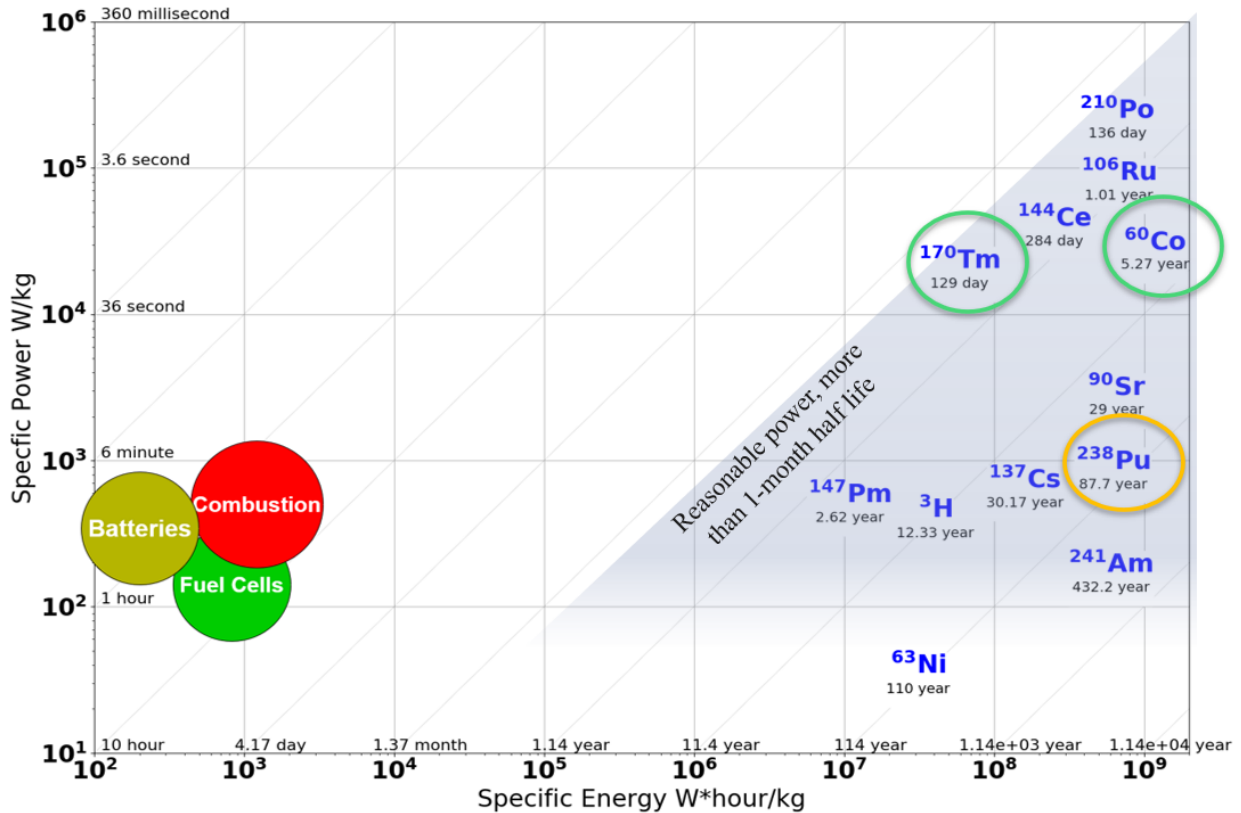


Figure 5: Radioisotope Energy and Power

There are differences in the total amount of energy stored with a radioisotopes (ranging from  $10^7$  to  $10^9$  Wh/kg), however the specific power W/kg is determined by both the energy and the half-life. A key point to understand is that isotopes with shorter half-lives will have a higher power density. Pu-238 and Co-60 have a similar amount of energy, however the shorter half-life of Co-60 means that energy is released over a shorter period increasing the power density by a factor of 30.

Because this is a NIAC report where fission, fusion, and antimatter are evaluated, it worth comparing radioisotopes to other high density power sources. Looking at Co-60 when it decays to Ni-60 the difference in mass of the two isotopes can be compared and the energy generated can be compared to antimatter. Cobalt-60 produces approximately 0.005 percent of antimatter. Using classical kinetic energy ( $\frac{1}{2}mv^2$ ) the maximum theoretical velocity of an atom of Ni-60 thrown with the energy of the Co-60 decay it would have a velocity of  $V_e$  of 0.7 percent of the speed of light.

Table 4: Maximum Theoretical Performance for Various Nuclear Energy Sources

	Reaction	Energy [% $mc^2$ ]	Exit Velocity [% c]	$\Delta V$ ( $m_o / m_i$ ) = 10 [%c]
<b>Cobalt-60 Decay</b>	2.6 MeV/decay	0.005	0.7	1.6
<b>U-235 Fission</b>	200 MeV/fission	0.091	3	6.9
<b>Fusion to <math>^{56}\text{Fe}</math></b>	8.5 MeV/nucleon	0.912	9.5	21

For an interstellar audience asking about speed. Radioisotope technology could achieve 1.6 percent of the speed of light, but a realistic high-performance number would be much lower. The Extrasolar Express aims to achieve 100 km/s which is about 0.033 percent of the speed of light. It is conceivable that could be increased to a couple hundred km/s and still be within the bounds of a credible engineering design.

Table 5 describes the relationship between radioisotope quantity, decay rate, and power.

*Table 5: Quantity, Decay, and Power Relationships*

	Equation	Description
Quantity	$M(t) = M_o e^{-\frac{\ln(2) t}{t_{hl}}}$	The number of atoms of Co-60 decays exponentially with time.
Decay Rate	$\frac{dM(t)}{dt} = -\frac{\ln(2)}{t_{hl}} M(t)$	The rate of decay (atoms/s) is proportional to the number of atoms. This can also be measured in Curies where 1 Curie = $3.7 \times 10^{10}$ decays/s.
Power	$P(t) = -E_d \frac{dM(t)}{dt} = \frac{E_d \ln(2)}{t_{hl}} M(t)$	The power is proportional to the decay rate which is also proportional to the number of atoms.
Where $M(t)$ is the quantity of Co-60 atoms vs. time, $M_o$ is the quantity of atoms at $t = 0$ , $t_{hl}$ is the half-life in seconds, $P(t)$ is power vs. time and $E_d$ is the energy per decay (2.6 MeV).		

There is a direct relationship between power and the quantity of radioisotope and number of Curies of radioisotope. Each gram of Co-60 is approximately  $1 \times 10^{22}$  atoms. This translates to  $4.2 \times 10^{13}$  decays per second. In Curies this translates to  $1.126 \times 10^3$  Curies of Co-60 per gram of Co-60. Each decay of an atom possesses 2.6 MeV of energy which translates to the 17.4 W/g of Co-60. In terms of Curies each Curie of Co-60 possesses approximately 15.4 mW of power.

The power level is purely based upon the number of atoms and the half-life and decays exponentially with time. After one half-life the power is half and after two half-lives the power is one fourth the original power. This means that radioisotopes are useful for up to a few half-lives. As a rule of thumb, the mission length should be on the order of the half-life or less. In cases where the mission is longer, the hardware must be designed to handle the variable power.

For radioisotope electric propulsion, the half-life problem is somewhat mitigated by the fact that the propellant is being used up while the power is decreasing which allows for a more constant acceleration.

Radioisotopes are blessed by the fact that the power produced by the radioisotope cannot be controlled. This is great from the perspective that no active control systems are necessary. In addition, the power is reliable. No matter the external conditions, we know exactly what power level will be over the entire mission. This makes radioisotope systems extremely simple and compact. In a fission system, significant resources are expended to evaluate reactivity control and control drums, reflectors, neutron moderators,

and control points all are needed to be highly designed operated and controlled to properly maintain the fission chain reaction.

## Generic Radioisotope Production

The production of radioisotopes requires a nuclear reaction between two particles. To create a radioisotope inside of FCM™ one of the following reaction pathways is required.

- **Neutron Reactions:** Neutron activation is the process of a nuclide absorbing a neutron and becoming radioactive (n,γ). There are other reactions such as a (n,2n) or (n,p). Low energy neutrons (0-1 MeV) can be produced in high flux fission reactors and higher energy neutrons can be produced by fusion (< 14.1 MeV) or using accelerators which can produce a very high energy tailored neutron spectrum albeit at a lower flux level.
- **Proton/Ion Reactions:** High energy proton, deuteron, and alpha particle reactions can interact with a nucleus to create radioisotopes through absorption, spallation, or other means.
- **Photon Reaction:** photonuclear reactions provide another set of possible atomic reactions that can produce new radioisotopes. Recent advances in electron accelerators can produce high-flux high-energy gamma environments through Bremsstrahlung radiation. Several methods for producing medical isotopes have been shown using this method.
- **Fission:** two radioisotopes are produced from a fission reaction. The exact radioisotope produced is dependent upon the nuclide being fissioned and the incident neutron energy. There are many heavy nuclei which are fissionable and will produce a different set of radioisotopes, providing many potential options for radioisotope production.

A cross section that describes the probability of the reaction process to occur. Reactions with larger cross sections are key to achieving a greater conversion fraction of the non-radioactive source material into a radioisotope in a shorter period of irradiation.

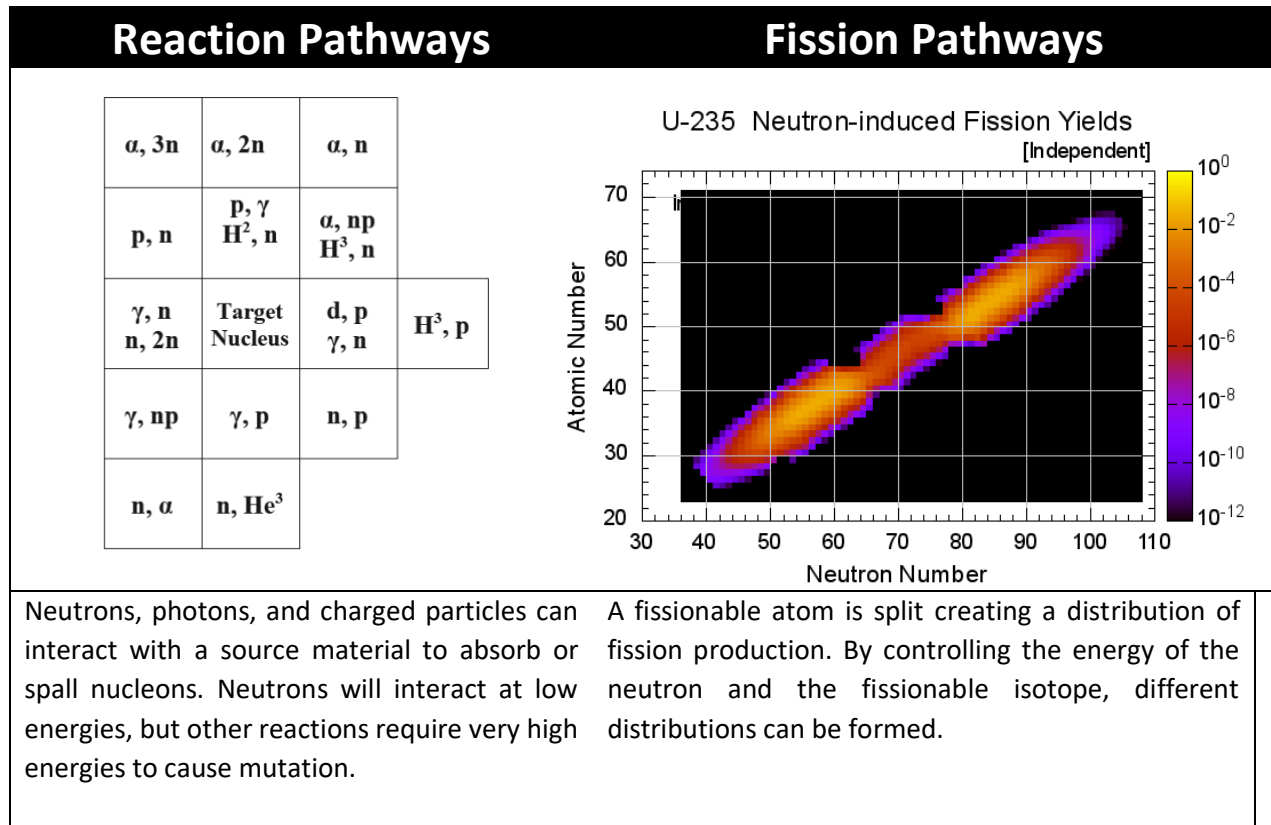


Figure 6: Comparison of Particle Reaction and Fission Pathways for Production of Radionuclides.

The cross sections require incident radiation. There are multiple possible radiation sources available:

- **Fission reactors:** currently available fission reactors can provide high fluxes of neutrons in thermal (energies around 0.253 eV) and to a lesser degree at higher energies up to 1 MeV. HFIR and ATR have produced isotopes such as Pu-238. For nuclear reactions that can be driven by low energy neutrons, fission reactors are excellent choices. Harvesting fission products is another method, but it is challenging in that many different isotopes are produced, which requires radiochemistry to process
- **Fusion reactors:** while fusion reactors are not break even in terms of their energy gain, currently available D-T fusion reactors can provide 14.1 MeV neutrons at a moderate flux. In some cases, fusion and fission can be combined into a hybrid reactor to provide a higher neutron flux.
- **Accelerators:** Accelerators are a well-known technology capable of accelerating charged particles to an incredibly high energy. Accelerators can provide a wide range of energies and can provide a beam energy tailored to the correct activation energy of the reaction desired. Accelerated protons, deuterons, and alpha particles can be used directly to produce many radionuclides. Accelerated electrons can produce predictable and controllable level of x-ray and gamma photons through Bremsstrahlung. These photons reactions can then be used to drive nuclear reactions and produce nuclear battery materials. Accelerators are very flexible, but usually suffer from low flux. However,

recent advances in accelerator technology from demand in the medical radioisotope industry have yielded potential production methods for significant quantities of radioisotopes.

Thermal neutron activation in a fission reactor is a mature radioisotope production method and is the basis of the EmberCore technology. There are existing facilities which can be utilized, and the radioisotope of interest can be produced in reasonable quantities.

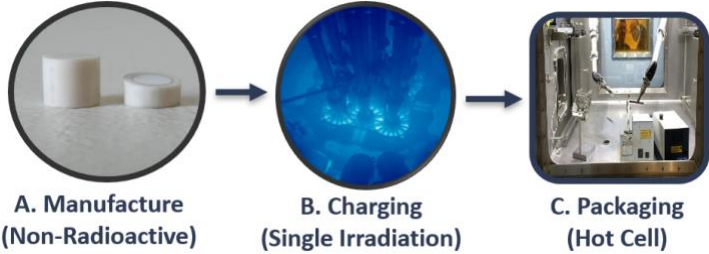
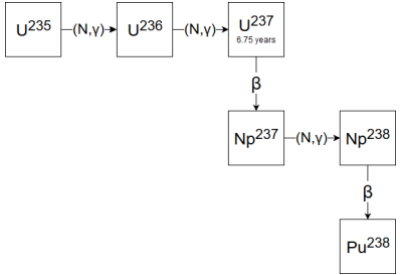
### 3. Enabling Technology – EmberCore™

USNC-Tech is proposing a game-changing power source technology called EmberCore<sup>11</sup>. When combined with other state-of-the-art and near-term technologies, this architecture can achieve this ambitious mission. An EmberCore power source can achieve a specific mass of 5-8 kg/kW<sub>e</sub> in a compact package. The spacecraft would be capable of delivering a 20 kg payload to 100 km/s of  $\Delta V$  over a 5 to 10-year timeline.

The key innovation USNC-Tech is utilizing is a novel manufacturing process for radioisotope power systems that unlocks the ability to produce high performing non-traditional radioisotope materials that can be produced cheaply and quickly compared to traditional Pu-238 radioisotope systems.

The EmberCore contains multiple small embers. These embers are first manufactured in a lab using naturally occurring, cheap, and non-radioactive precursor materials. The precursors are then "charged" inside of a reactor, activating them into the desired radioisotope. Then the target is packaged into an EmberCore package for the customer. This production process is greatly simplified compared to Pu-238 as it is a "charge and go" process and doesn't require radiochemical processing or multi-step irradiation procedures in Table 6.

Table 6: Pu-238 vs. Ember Manufacturing



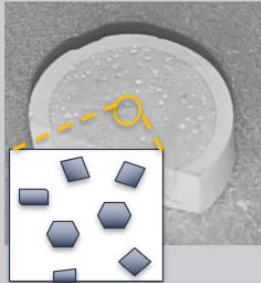

Ember Manufacturing Process	Pu-238 Process
 <p><b>A. Manufacture (Non-Radioactive)</b> → <b>B. Charging (Single Irradiation)</b> → <b>C. Packaging (Hot Cell)</b></p>	 <pre> graph TD     U235[U-235] -- "(N,Y)" --&gt; U236[U-236]     U236 -- "(N,Y)" --&gt; U237[U-237 6.75 years]     U237 -- "β" --&gt; Np237[Np-237]     Np237 -- "(N,Y)" --&gt; Np238[Np-238]     Np238 -- "β" --&gt; Pu238[Pu-238]           </pre>
<p>The ember is manufactured using common non-enriched, non-radioactive materials and then "charged" through a single neutron activation in a fission reactor. No radiochemistry separation.</p>	<p>This process requires multiple activations, separation processes and waiting periods involving special nuclear materials that are in short supply.</p>

There are multiple radioisotopes that can be produced in an ember (ex. Co-60, Tm-170, etc.). This allows for the radioisotope to be tailored by enabling customers to match their heat source with their mission duration, power level, and radiation tolerance. USNC-Tech is commercializing this ember technology for both terrestrial and space applications.



## Encapsulation Safety

The built-in encapsulation capability of ember technology both improves the safety case and simplifies the manufacturing process. Embers are composed of two different ceramics. The nuclear precursor ceramic contains a material which when exposed to a radiation field activates into the desired nuclear ceramic. The precursor is surrounded by the encapsulation ceramic. The encapsulation ceramic is composed of a well-characterized structurally and chemically stable ceramic. In most cases the encapsulation ceramic is a single encapsulation, however additional layers of encapsulation are possible as shown in Figure 7.

No encapsulation	Single Encapsulation	Double Encapsulation	Triple+ Encapsulation
			
Radioisotope Only	<b>Wall Encapsulation</b>	Wall & Matrix	Wall, Matrix & Coatings
Traditional approach, only precursor material, no encapsulation	Dual ceramic pellet with encapsulation material forming a wall around the inner precursor filling	Inner filling is composed of um scale precursor particles surrounded by nm scale power forming a second encapsulation	A solgel or similar process to create a microscale precursor kernel and apply additional encapsulations coatings

*Figure 7: Ember Encapsulation*

The encapsulation material is chosen as a well known ceramic that can withstand the intense environment inside of a nuclear reactor. As the precursor material activates it may lose structural properties, however the encapsulation ceramic serve as a structural element and maintain strength throughout irradiation. This design is inspired by the design of nuclear fuel technology.

USNC has developed a fission fuel technology, fully encapsulated ceramic matrix (FCM™), which isolates TRISO-like fissile nuclear fuel in a refractory carbide matrix. The FCM™'s resistance to fission product diffusion, mechanical stability in high fluence, and high temperature tolerance provide an excellent safety case to regulators facilitating the licensing of the MMR™ nuclear reactor being developed by USNC. The FCM™ carbide matrix is designed to fully encapsulate fissile material and all radioactive byproducts in a fission reactor under all normal and accident scenarios over the 20-year lifetime of the reactor. This provides a strong safety basis upon which expedites licensing processes. This technology, for the same reasons it is compatible for terrestrial fissile fuels, also offers the ability to fully contain radioisotopes for energy storage for the EmberCore technology.

## Ember Fabrication

USNC-Tech has done extensive material development focused on Thulia based embers with encapsulation in SiC and Al<sub>2</sub>O<sub>3</sub>. A simplified process for fabricating and charging embers is shown in the fugure below.

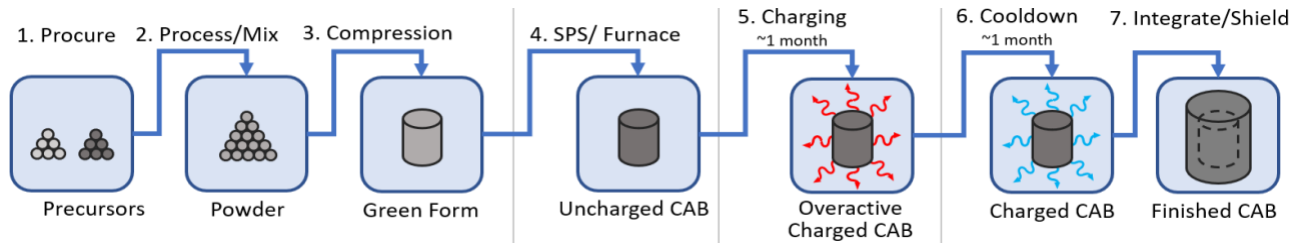


Figure 8: Ember Fabrication and Charging Process

Extensive work has been done in powder processing, forming, and sintering embers. Much of the detailed work is considered proprietary and not included in the public version of this document. For this Phase I NIAC some basic work was done on producing CoO based embers encapsulated in  $\text{Al}_2\text{O}_3$ . Work was completed looking at phase properties, additives, binding, and powderprocessing. A few prototype Cobalt embers were sintered. As shown in Figure 9.

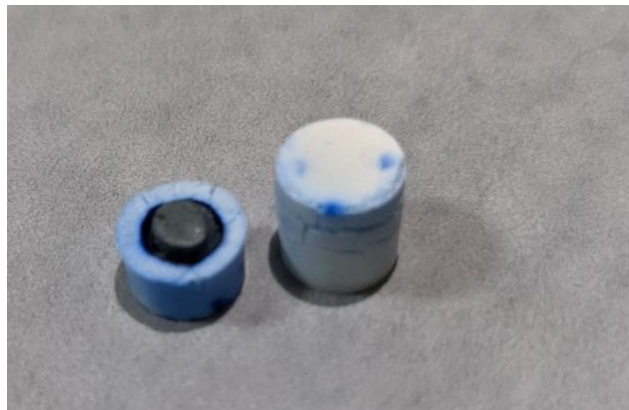
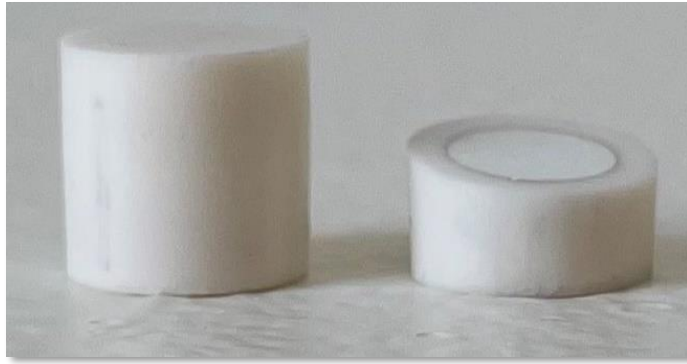


Figure 9: Prototype CoO Precursor and  $\text{Al}_2\text{O}_3$  Encapsulation Embers.

The CoO has a deep blue pigment. The prototype embers suffered from cracking due to uneven sintering of the two materials. A clear solution to this uneven sintering is seen by the team as a process of refining powder treatments, sintering aids, furnace heat application curves, and pressing methods for the multi-step forming process. This work was promising on limited resources and we a higher quality ember can be produced which would be irradiated in a Phase II NIAC.

It is worth noting that USNC-Tech has going though a similar process maturing the  $\text{Tm}_2\text{O}_3$  based embers as shown in Figure 10. The Tm based embers have been matured to the point that they are currently being irradiated in low power facilities and are undergoing safety analysis for a high power irradiation. The development pathway for CoO is seen as very similar.



*Figure 10: Thulia Alumina Embers.*

## Criteria for Pre-Activation Encapsulation and Charging of Radioisotope

When selecting a precursor material and associated activated radioisotope, there are several key metrics of interest that are discussed below:

### Precursor Selection

- **Thermal neutron absorption cross section:** cross section of around 30 barns or above are good for fast production rates inside of fission power systems.
- **High temperature and chemical stability:** the radioisotope should be able to withstand high temperatures preferably above 1500 K to withstand the sintering process and provide operational temperature margin. The radioisotopes can typically be bonded as an oxide, nitride, or carbide to increase the operations temperature. Phase changes and chemical compatibility are also a concern.
- **Natural abundance of target precursor isotope:** Some natural elements have several isotopes each with their own cross section and activation isotopes. The target isotope should be relatively abundant.
- **Toxicity:** Precursor isotopes should be relatively easy to work with in terms of their chemical toxicity.
- **Double activation considerations:** if the thermal neutron cross section of the converted radioisotope is large, it will transmute into another radionuclide typically with a mismatched half-life. The cross section of the radioisotope should be relatively small to reduce transmutation loss of the desired radioisotope in the activation process.

### Encapsulation Material Selection

- **Low absorption cross section:** the encapsulation materials should have a small absorption cross section to allow for neutrons to travel inside into the precursor material
- **Short lived or no activation production:** one major purpose of the encapsulation layer is to keep the radioactive material contained, so it should not produce significant activation products itself or if it does they should be short lived such that they can decay away quickly before the device is deployed.
- **Well known nuclear materials:** the encapsulation material should have well known thermal and structural materials and how those properties change as a function of reactor fluence and irradiation temperature should be well known.

- **High temperature and chemical stability:** the encapsulation material should have a high temperature capability greater than or equal to the precursor material and shouldn't chemically interact with the precursor material during sintering, activation, or during operation.
- **Good thermomechanical coupling:** the thermomechanical couple of the precursor and activation materials should be well designed. During dimensional changes such as thermal expansion, activation swelling, or material decay the encapsulation of the material should be maintained. This can be accommodated by both careful selection of materials and by design of the ember to accommodate interface regions. For example by designing a small gap large enough to accommodate swelling or by using a low modulus material such as porous graphite to have a crumple zone.

### Activated Product Performance Characteristics

- **Radiation type and energy (alpha, beta, gamma):** Traditionally, radioisotopes have been alpha emitters. Alpha emitters deposit their energy over a very short distance and do not produce x-rays. Alpha emitters tend to be actinides and are often special nuclear materials. There are a significant number of attractive beta emitters, however beta emitters produce a significant number of x-rays while slowing down. Higher energy beta emitters produce higher energy gamma-rays. Some beta emitters also produce gammas. Gamma emitters typically produce hard gamma rays but can often have very high-power density. High energy gammas are very difficult to shield
- **Half-life:** The half-life of the radioisotope should be about twice the mission duration. Too short of half-life and the power source will decrease greatly in power over the mission, too long and the power density will decrease.
- **Regulatory limitations:** As will be shown later in the regulatory section, there are limitations on the absolute power for each radioisotope in the context of launch approval.
- **Mass:** The mass of the radioisotope material is typically very small, on the order of grams as most radioisotopes of interest produce greater than one watt per gram. The encapsulation is usually on the order of hundreds of grams. Depending on the radioisotope and the need for shielding, the mass of the shield can be anywhere from zero to multiple kilograms for a watt-scale nuclear battery.

The equation below governs the production rate of the activated radioisotope from the precursor.

Activation Isotope Production Governing  
Equations

$$P(t) = \int^V \int_0^\infty N(\mathbf{r}) \Sigma_{x \rightarrow N}(E, \mathbf{r}) \phi_x(E, t, \mathbf{r}) dE dV$$

$$L(t) = \frac{\ln(2) M(t)}{t \frac{1}{2_N}} + \int^V \int_0^\infty M(\mathbf{r}) \Sigma_{x \rightarrow M}(E, \mathbf{r}) \phi_x(E, t, \mathbf{r}) dE dV$$

$$\frac{dM(t)}{dt} = P(t) - L(t)$$

Where  $P$  is the production rate of the desired activation nuclide  $M$ ,  $L$  is the loss rate  $M$ ,  $E$  is the energy dependence,  $r$  is the spatial dependence,  $N$  is the atomic density of the precursor material,  $\Sigma_x(E, r)$  is the production cross section,  $\phi(E, t, r)$  is the radiation source particle flux, and  $t_{1/2N}$  is the half-life of the product nuclide.

### Isotope Selection and Target Design for Co-60

An exhaustive trade study looking at production of different radioisotopes taking into their performance and ease of manufacturability. The results of this trade study informed the original NIAC Phase I proposal submission utilizing Co-60 for the Extrasolar Express mission. Cobalt checks most of the boxes for performance and ease of manufacturability. The 5.27 year half-life is in the sweet spot for a mission envisioned to take 5-15 years to complete. The power density of Co-60 is incredible, possessing 31 times higher maximum power density compared to Pu-238.

*Table 7: High Power Density Radioisotopes*

Isotope	Ideal Power Density [W/g]	Half-Life [year]
<b>Tm-170</b>	11.5	129 days
<b>Co-60</b>	17.4	5.27
<b>Pu-238</b>	0.56	87.4

Cobalt is one of the most straight forward isotopes to produce. Natural Cobalt has only one isotope Co-59. Co-59 readily bonds with oxygen and has high temperature compounds. CoO has a melting point of 2208 K and through proprietary compounding methods the melting temperature can be further increased. There are multiple encapsulation materials available, but for the Phase I NIAC study alumina was the focus.

Co-59 has excellent activation characteristics. The relatively small 30 barn activation cross section requires a high flux reactor; however, the low cross section is beneficial for producing large quantities of material as the material doesn't self-shield and a significant number of targets can be loaded into a reactor without reducing the reactivity significantly. A key advantage of Co-60 is that its neutron absorption cross section is extremely small. As the Co-59 is transmuted into Co-60, the Co-60 is not transmuted into another undesired product.

The relatively long half-life of Co-60 provides some benefit as well. With shorter lived radioisotopes such as Tm-170 there is a logistical need to produce and utilize the material before it decays. The longer half-life allows for flexibility in the production with various reactor partners with different cycle lengths and flux levels.

All these key features are boons to produce Co-60. The radioisotope is flexible and not restricted to a specialized reactor for production. This is a key supply chain advantage against other activation-based isotopes which requires a specific flux level and irradiation time, often limiting their supply chain capability. Figure 11 below shows the production of Co-60 in Oak Ridge National Laboratory's High Flux Isotope Reactor (HFIR).



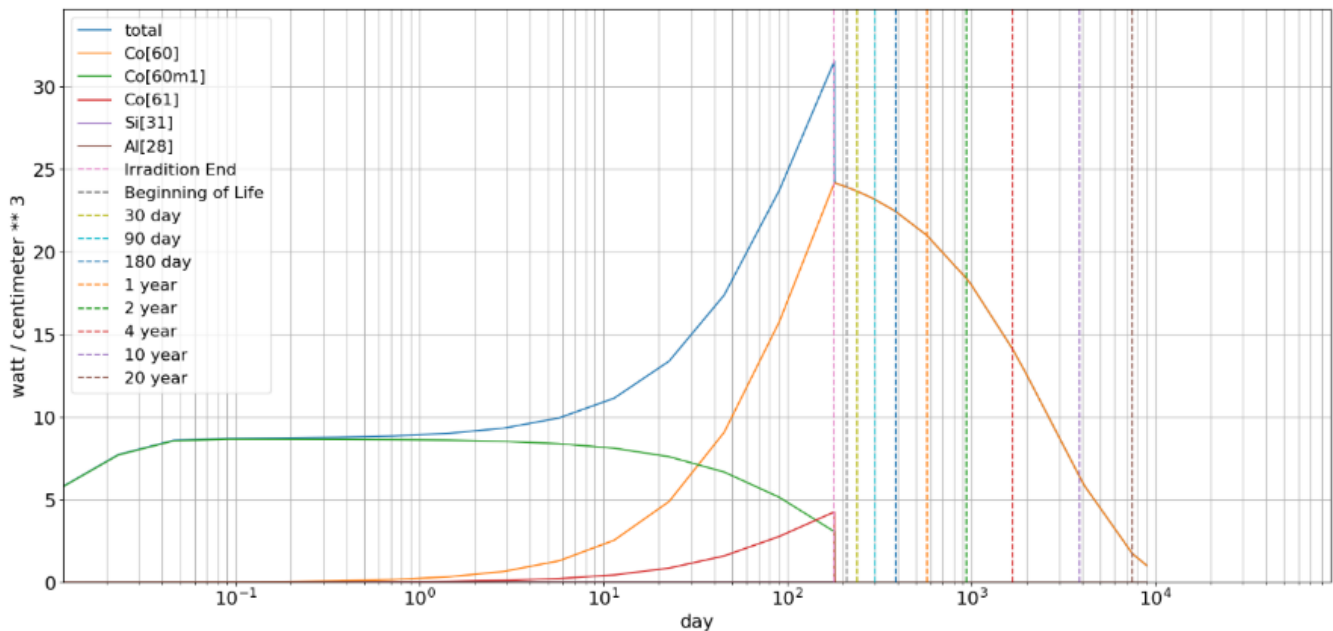


Figure 11: Top: Power Graph for a 6-month 50 Volume Percent Cobalt Oxide 50 Volume Percent SiC Ember in the Oak Ridge HFIR reactor with a neutron flux of  $4.5 \times 10^{15} \text{ n/cm}^2\text{-s}$ . Analysis Completed with ORIGEN

Note that HFIR irradiation cycles are approximately 23 days long and have maintenance periods between cycles of a few weeks to a couple months. The irradiation should in reality be stretched over 8 cycles over a year to a year and a half. There would be some appreciable decay, but relatively small.

As mentioned before Co-60 has a small absorption cross section so it is not susceptible to double activate conversion after production. Each 23.5-day HFIR cycle converts approximately on average 5.5 percent of the Co-59 into Co-60. At the end of the process each ember has a power density of approximately  $24 \text{ W/cm}^3$  or approximately  $4.8 \text{ W/g}$  of power in the ember. The ember is composed of only 50 percent by volume Co-60 the power density of the Co-60 region is approximately  $50 \text{ W/cm}^3$ . Over these 8 cycles approximately 44 percent of the Co-59 is converted into Co-60. This fuel spec of  $4.8 \text{ W/g}$  in the ember was used for the Extrasolar Express Mission.

While the activation analysis was focused on HFIR, any reactor that matches the thermal neutron fluence would produce a similar result if the production period happened over a period relatively short compared to the half-life of Co-60. For example, a 2-year irradiation in a power reactor with a flux of  $1.25 \times 10^{15} \text{ n/cm}^2\text{-s}$  would yield a similar product.

A concern about target irradiation is self-shielding. If the cross section of the material being activated is too large, then the material becomes “black” and the neutrons are absorbed in the periphery of the

material and are not absorbed evenly in a process known as self-shielding. Figure 12 evaluates the self-shielding based on an MCNP calculation of the HFIR reactor in the VX7 irradiation positions.

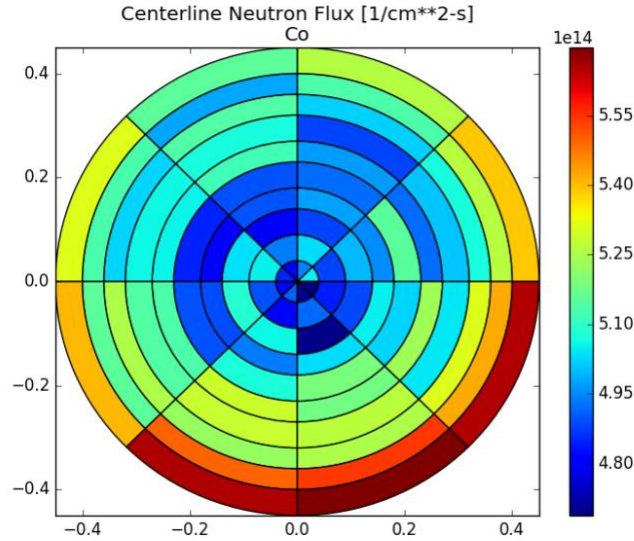
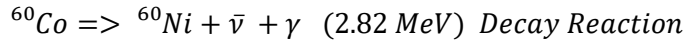
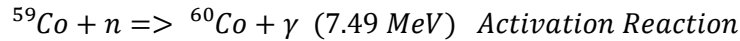


Figure 12: Self Shielding Analysis

The ember target is 8 mm in diameter with a CoO precursor. The key takeaway here is that the flux in the center region is reduced only marginally from the flux in the outer region (a maximum of 15 percent). This means that the target is getting even activation.

There can also be thermal concerns during production. The 24 W/cm<sup>3</sup> does require cooling during production, however the energy produced by the (n, γ) activation reactor is greater than the decay power.



In addition, every atom of Co-60 produced is produced in the activation cycle which is shorter than the half-life, whereas the decay of Co-60 takes place over the course of the period of the half-lives. What this means is that during the activation process, the power produced by activation will be much greater than decay heat. So, a highly activated ember will only produce marginally more heat during the activation process compared to a fresh ember. Furthermore, during activation additional energy from neutrons slowing down or gammas emitted elsewhere during irradiation can increase the heating. Looking at ember target design from a thermal perspective, the thermal heat production during activation of 7.49 MeV per Co-60 atom produced. This translates directly to a heating rate  $q'''$ .

$$P_{\text{activation}} \approx P_o \frac{t_{1/2}}{t_{\text{activation}} * \ln(2)} * \left( \frac{Q_{\text{activation}}}{Q_{\text{decay}}} \right) = 24 \frac{\text{W}}{\text{cm}^3} * \frac{5.27 \text{ year}}{\ln(2) 6 \text{ months}} * \left( \frac{7.49 \text{ MeV}}{2.82 \text{ MeV}} \right) = 969 \frac{\text{W}}{\text{cm}^3} \gamma \text{ heat}$$

It is important to note that the 7.49 MeV activation gamma is only deposited semi locally. The actual gamma energy is composed of a cascade of higher and lower energy gammas as defined by databases of prompt gamma from slow neutrons. Many of the higher energy gammas will escape out of the ember

during activation. Due to the high heating rate, it is imperative to closely consider the thermal conditions of the ember. If the temperature peaking is too high, the diameter of the ember can be reduced, higher thermal conductivity can be found, or the activation flux decreased. In general, the thermal conditions of activation may be more challenging than during operation. In addition, fluence and temperature affect the response of the nuclear material especially when dealing with dimensional changes. Most ceramics have reduced swelling within a certain temperature range. For alumina temperature above 400 degrees C are desirable.

## X-Ray and Gamma-Ray Shielding

As a percentage, the vast majority of the Bremsstrahlung x-rays (from beta particle attenuation within the ember) deposit their energy locally within the embers. The biggest drawback to Co-60 is the gamma rays that are emitted following beta decay. These gamma rays are likely to escape the embers without depositing energy and, thus, require shielding to protect personnel during integration and sensitive electronics during the mission. Figure 13 shows the x-ray emissions for Co-60.

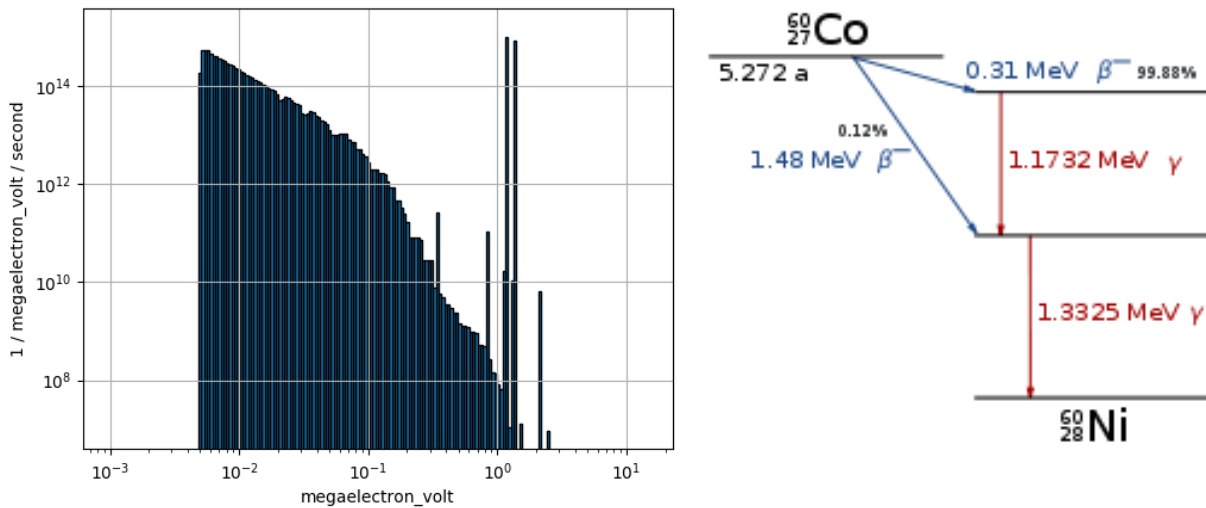


Figure 13: Left: Photon Spectrum for Cobalt Ember from ORIGEN. Right: Decay Scheme for Co-60.

The decay scheme on the right show how the majority of Co-60 decays emit two gamma rays (1.17 MeV and 1.33 MeV). There is also a very low probably 1.48 MeV beta decay and a very high probability of 0.31 MeV beta decay. (These beta energies are the maximum possible energy in the beta spectrum; the mean beta energy is approximately one-third of the maximum energy.) The 1.48 MeV beta is too low of probability to cause concern and the 0.31 MeV beta is very easy to shield. The two gamma rays, however, are produced in significant quantities and post a shielding challenge. In the left image, the photon spectrum is shown for the ember from Figure 11. This spectrum includes the SiC encapsulant material and impurities in the materials, but their contribution to the photon spectrum is negligible. The two peaks on the right side are the two gamma emissions from Co-60. For Co-60 approximately 2.6 MeV of energy is produced per decay (the energy of the two gammas plus approximately one third of the energy of the betas as two thirds of the beta energy is taken out of the system by the anti-neutrino emitted in a beta decay). Table 5: Quantity, Decay, and Power Relationships

The energy, again, is largely released in the form of the two gamma rays. These gamma rays attenuate with both distance and material shielding. There are four major ways to deal with shielding x-ray radiation.

- **Distance:** Dose rate is reduced by increasing the distance between the radiation source and the sensitive components.
- **Shielding:** Shielding attenuates radiation intensities and, thus, reduces dose rate. The principal absorption mechanism between 100 keV and 10 MeV is Compton scattering with orbital electrons. Due to their higher electron density, heavy metal shields require the smallest thicknesses/masses to stop high-energy photons. Natural or depleted uranium metal is the best naturally occurring element for this reason. Tungsten is a reasonable second choice and sometimes could be preferable for its high melting temperature and robust material properties.
- **Time:** Dose is reduced by limiting the amount of time that people or sensitive components are exposed to radiation. This is particularly beneficial in the case of personnel.
- **Radiation hardening:** Increasing the tolerance of a material to x-ray radiation can be an effective strategy. Typically, commercial grade radiation tolerant components can withstand 25 krad of radiation. Radiation hardened components are capable of withstanding 100 krad and, for some components and applications, more than 1 Mrad level. For example, the Juno spacecraft's computer was designed to tolerate an astounding 50 Mrad to protect against Jupiter's ionosphere.

The radiation shield is made from depleted Uranium because it is the best available shielding material. The Tenth Value Layer (TVL) for shielding the 1.17 MeV and 1.33 MeV gamma rays from Co-60 is about 2 cm. TVL is the thickness required to reduce the intensity by an order of magnitude. The shield is designed to provide, at most, 5 rem/hour of dose at 30 cm. This dose rate is below the NRC definition of a radiation area and is similar to the dose on the ISS. (Further efforts with Time, Distance, Shielding principles would still be employed to make dose rates to personnel As Low As Reasonably Achievable.) This shield design would be safe for ground crews to operate in proximity for extended periods of time (tens of hours). The analysis was completed using a 1D spherical geometry deterministic code called SAS1D in the Scale code suite and included an inner region composed of embers according to their power density, a thin tungsten housing, and an outer region of the depleted uranium shielding. The results in Table 8 show that mass of shielding required for a mission is not linear and larger power levels benefit from reduced mass per unit power.

*Table 8: Shield Design for 5 mrem/hour Dose Rate (1D Analysis).*

Co-60 Power	Shield Thickness [cm]	Full Shield Mass [kg]	Mass Per Unit Power [kg/kW <sub>th</sub> ]
1 W	13.2	350	350000
100 W	15.8	1060	10600
1 kW	16.8	2340	2340
100 kW	19.2	3050	30

In the case of shielding mass, there are a few key concepts to understand. Shielding material attenuates the high-energy photons in an exponential fashion. However, there is also a strong geometric effect that reduces

dose by increasing size, where dose is inversely proportional to the radius squared. The mass, however, is proportional to the radius cubed. The shield is not the only component that attenuates photons and, at higher powers, the embers themselves serve to block some of the photons emitted by other embers. Gamma rays require multiple collisions, which is usually represented by a buildup factor in a hand calculation, but for this analysis the SAS1D employs a multigroup energy transport method.

Based on the results, when looking at mass there is a clear trend showing that the shield mass per unit power decreases substantially as power increases. This does show that higher power will yield better performance.

The 19 cm shield will provide a  $4 \times 10^{12}$  reduction in intensity (not accounting for gamma-ray self-absorption and geometric attenuation) enabling for safe transit to the launch site and handling by ground crews.

Another key concept of the NIAC to understand is that this shield is designed for ground crews and launch safety. Humans are by far the most sensitive to radiation and, once in space, the vast bulk of the shield can be ejected and a small shadow shield and perhaps some spot shielding on sensitive components is all that is necessary for ensuring electronics safety.

### Supply Chain and Production

A key concern with radioisotopes is production. Looking at Pu-238 the supply chain has been a key limitation. Refer to Table 6. For Pu-238, a precursor is required called Np-237. Np-237 is itself a special nuclear material that is obtained by processing spent nuclear fuel. The process for obtaining Pu-238 from Np-237 has multiple steps involving an activation into Np-238. The Np-238 has a 2.1-day half-life to decay to Pu-238. Only a few percent of the Np-238 is converted and the Np-237 must be recovered. In addition, the Np-238 has a 2000 barn fission cross section (very large) which means that a significant amount of the Np-238 is fissioned before it decays to Pu-238 and care must be taken to provide the correct flux level to optimize the production cycle. The complexity of the Pu-238 activation process requires:

- Significant radiochemistry facilities
- Require reactors to operate in short irradiation cycles and flux levels, limiting the number of production facilities
- Requires facilities to be licensed to possess special nuclear materials

These challenges limit the production capability for Pu-238. While Pu-238 is an excellent radioisotope and enabling for many missions, only approximately 1.5 kg of material can be produced a year (approximately 750 W per year of production) and increasing that supply chain would be challenging without building new facilities.

The medical and industrial industry has been producing Co-60 in significant quantities over the last five decades. Co-60 is produced in greater than 100 kW quantities per year. Co-60 has fallen out of favor for cancer treatment in developed countries typically losing market share for proton accelerators. However, in underdeveloped countries, Co-60 use is increasing, and the net effect is that Co-60 production is on the rise. Canadian CANDU reactors produce Co-60 in great quantities and traditional pressurized water reactors are also being utilized to a lesser degree. The key message here is that existing facilities can produce significant amounts of Co-60 in kW-scale quantities and that additional capacity is available to produce Co-60.



Early on in this Phase I study a literature review was conducted looking at what had been proposed in the past with Co-60 production. One of the most influential papers was “Cobalt-60 Production at Savannah River” by H. F. Allen. This report detailed the Co-60 production at Savannah River in the 1955- 1962 timeframe over 4 million curies (65 kW) of Co-60 was created for medical and industrial uses. The paper estimated that up to 8 million curies (130 kW) of Co-60 could be produced per year using an existing high-power reactor, but that many tens of millions of Curies could be produced some changes were made to the existing reactor. The paper also claims a cost of less than 50 cents per Curie in 1964 dollar which today would be close to 5 dollars per Curie in 2022 dollars. This would suggest that a 100 kW quantity could be produced for roughly 30 million dollars.

When evaluating production capability withing a reactor there are multiple factors to consider. The fundamental currency of the production capability is neutrons. A neutron can either be used to sustain the fission chain reaction or be used to produce a radioisotope. Inherently in the process there is wasted neutrons that either escape the system or are absorbed in a reaction that causes neither fission nor capture in the precursor material. Even worse are neutrons that are captured in the activated material, further activating the material into an undesirable radioisotope (luckily for Co-60 this is not a major concern).

This currency of neutrons means that reactor with higher power and higher reactivity are better for producing nuclear material. There are approximately 2.41 neutrons produced per fission in a U-235 based fission reactor. Each fission produced a fixed amount of power (roughly 200 MeV) so there is a direct linear relationship between power and available neutrons. Of the 2.41 neutrons per fission only a fraction of a neutron is available based on the excess reactivity (related to the excess number of neutrons) of the reactor. Most reactors have an excess reactivity which is less than one tenth of a neutron (this can be estimated from the six-factor formula from nuclear textbooks assuming an excess reactivity capability of 15 dollars). So, a rule of thumb would say that each fission can contribute 0.1 neutrons to radioisotope activation. This would mean that a 100 MW<sub>th</sub> reactor could for example contribute  $3.1 \times 10^{17}$  activation neutrons per second which would translate to approximately  $1 \times 10^{25}$  Co-60 atoms/year. That would further translate to 17 kW<sub>th</sub> of Co-60 per year. A GW scale reactor could produce GW scale quantities of radioisotope.

A key challenge to the EmberCore Technology is supply chain - scaling to produce kW-scale quantities of Co-60 embers. USNC-Tech has evaluated the supply chain and has talked with different irradiation service providers. Currently the medical radioisotope industry produces over 100 kW<sub>th</sub> of Co-60 each year. The production is done in power reactors. These large power reactors have business units to sign deals for reactor production. Before we can utilize the power reactors, we need to prove our technology with research reactors. Research reactors cannot produce in quantity but are willing to conduct experimental research. As previously mentioned, these research reactors are already engaged with USNC-Tech on Tm-170 production and are onboard with Co-60 production.

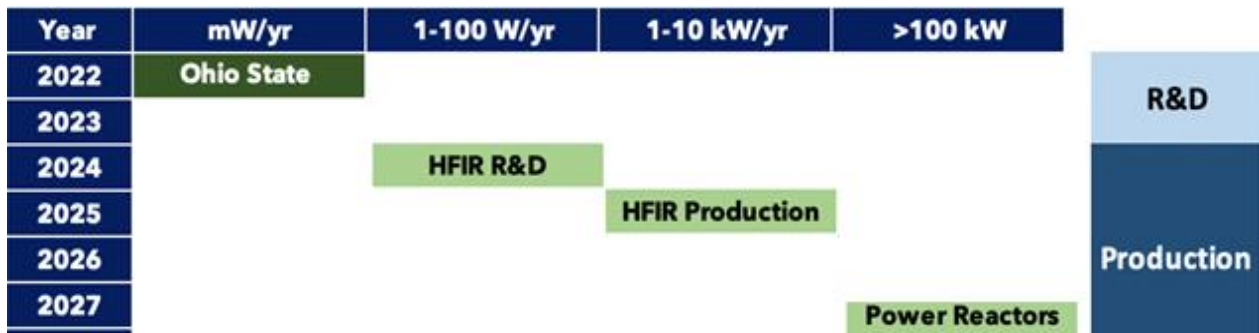


Figure 14: Envisioned Supply Chain Growth.

After production of Co-60 embers, transportation, device assembly, and storage logistics are necessary. For production of up to a few kW, existing facilities such as those at HFIR can be utilized under contract. However, larger scale production would require a dedicated integration facility.

### EmberCore Commercial Product for Lunar Market

USNC-Tech is developing a minimum viable EmberCore product, a simple radioisotope heating unit for the lunar market with a deployment goal of 2024. The same technology behind this product is utilized to enable the extra-solar mission utilizing a different radioisotope. It is worth discussing the commercial product and how USNC-Tech's internal development efforts on the product support the extrasolar mission.

The ability to endure long-duration exposure to darkness and extremely low temperatures is critical to establishing and maintaining a sustainable presence on the lunar surface. NASA's lunar exploration programs (such as Artemis and CLPS), depends on the ability of lunar systems to operate through lunar nights and within permanently shadowed regions (PSRs). USNC-Tech has been preparing a commercially procurable radioisotope heater unit (RHU), EmberCore, that will protect landers, rovers, and other surface assets from the dangerously low temperatures of the lunar night and PSRs. These assets are exposed to extreme cold and having a simple heater can maintain critical systems (such as chemical batteries and integrated circuits) during the night.

The embers are composed of an inner nuclear chargeable ceramic (NCC) and an outer inert ceramic as shown in Figure 15. The outer ceramic provides encapsulation for the radioisotope during production. A second layer of encapsulation is provided by the housing. A third encapsulation is provided by the x-ray shield. Finally an aeroshell is integrated which provide protection from re-entry heating. These encapsulation layers provide a robust and redundant safety system to protect accidental release of radioisotope material in the event of a launch failure.

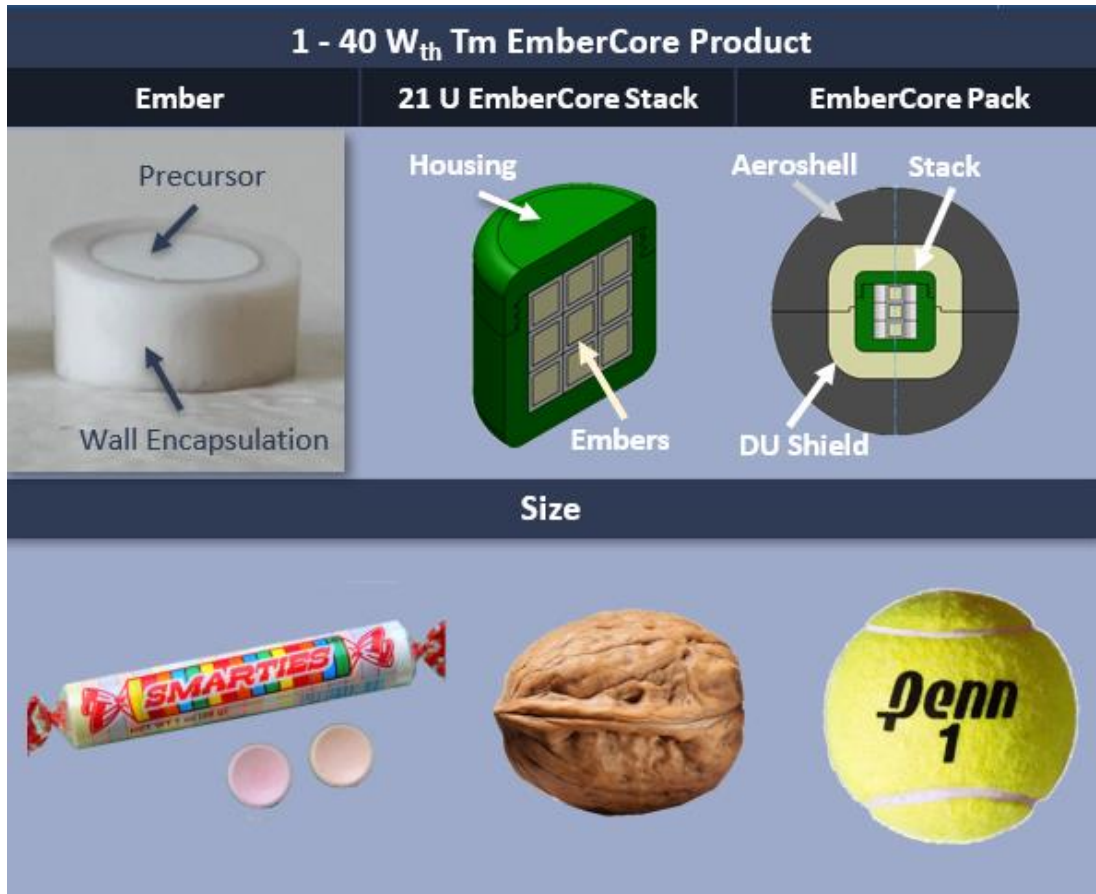


Figure 15: Left 1 - 40 W<sub>th</sub> EmberCore System

Surviving the lunar night is only the nearest term application for this EmberCore. Future commercial applications are numerous and include marine applications for long duration autonomous underwater vehicles for exploration and monitoring, and as x-ray sources for industrial, remote sensing, and medical applications. It is worth noting that the NIAC Phase I played a strong role the commercial development of the lunar product.

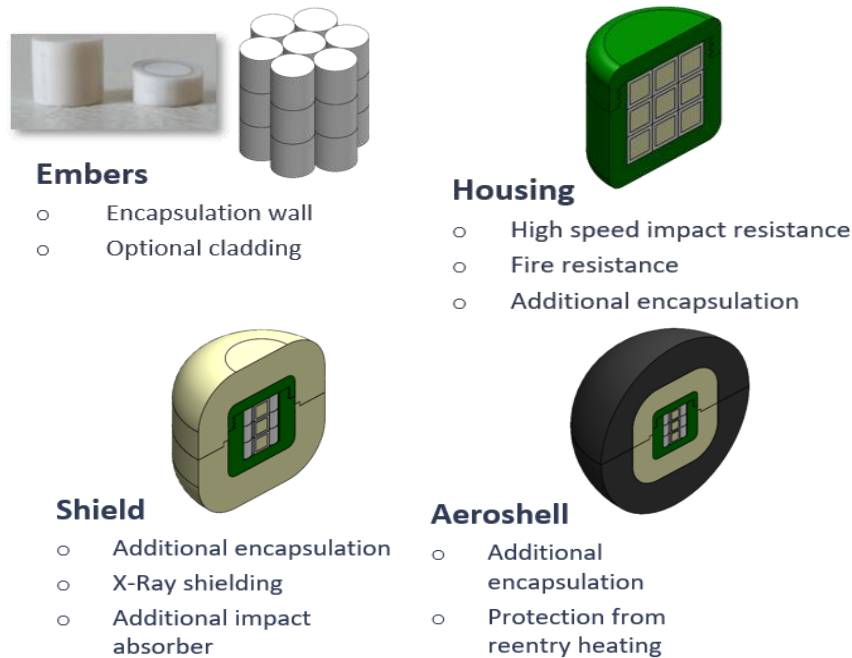


Figure 16: Safety Features of the EmberCore Technology

## 4. Regulatory and Launch Safety

Launch Safety is a key aspect of this Phase II proposal. It was found in the Phase I NIAC that the key challenge with developing the EmberCore technology is launch approval and regulatory licensing. Previous reviewers on the NIAC Phase IB proposal have also noted this, and a large scope of the future proposed work is dedicated to demonstrating regulatory feasibility.

### Ground Licensing

Co-60 is a radioisotope, and some have commented on the potential for use as a dirty bomb. However, it is important to note that Co-60 and many other isotopes have been used safely for many decades under federal and state regulatory licensing programs.

Co-60 has been produced for several decades in kW quantities for medical treatment so there are existing precedents for storage for this material in places such as hospitals. Regulators have established accountability through the 10 CFR Part 30 rules which mandate the requirements for a possession license to hold the materials including things such as a radiation safety program.

The ground licensing requirements for EmberCore are well-known and actionable. USNC-Tech has engaged with the NRC and the proper agreements states. USNC has a Part 30 license that USNC-Tech is amending to meet the needs of EmberCore.

- **Possession License:** Establishing radiation safety program and QA to possess radioisotope sources above exempt quantities for a 10 CFR Part 30 license.
- **License for Radioisotope Container:** Sealed source licenses for assembly of embers into EmberCore.

- **Transportation:** DOT transportation cask between integration facilities
- **Launch Vehicle Integration:** Established spacecraft integration conops and radiation worker strategy

NRC/DOT Licensing – Irradiation Facility to Launch Pad	
1.	<b>Ember Unit Irradiation:</b> Activation of CAB Units
2.	<b>Cooling Pond:</b> move irradiation capsules to temporary cooling pond storage
3.	<b>Transport to Hot Cell:</b> moving irradiation capsules to a hot cell possibly off-site involving a specialized container.
4.	<b>Hot Cell CAB Pack Integration:</b> Integrating the CAB Units into a stack/pack with x-ray shield.
5.	<b>Non-Hot Cell CAB Pack Integration:</b> Additional integration with parts such as the aeroshell and thermal interface.
6.	<b>Transport to Launch Site:</b> Transporting the CAB pack to the launch site
7.	<b>Integration and Transport on Launch Site:</b> Transporting and integrating the CAB pack on the launch site grounds
8.	<b>Integration with Rocket:</b> Integrating the CAB pack into a payload on the rocket

Figure 17: Simplified Ground Licensing Conops.

## Space Licensing

The basis for launch approval is the 2019 National Presidential Security Memorandum 20 which established a tiered system summarized in **Error! Reference source not found..Error! Reference source not found..**

Table 9: Launch Tier System Summary.

Tier	Radioisotope Quantity	Fission	Exposure Requirements (Public Dose in TED)	Probability of Occurrence	Scope
I	< 100,000 A2 <sup>(1)</sup>	N/A	0.025 – 5 rem	≤ 1 in 100	Review and approval process simplified
			5 - 25 rem	≤ 1 in 10,000	
			> 25 rem	≤ 1 in 100,000	
II	> 100,000 A2 <sup>(1)</sup> > Tier I	HALEU	5 rem to 25 rem	<sup>3</sup> 1 in 1 million	Significant cross agency review
III		HEU	> 25 rem	<sup>3</sup> 1 in 1 million	Significant cross agency review and presidential approval

A key regulatory determinant to the design is the difference between a Tier 1 and Tier 2 launch. A Tier 2 launch requires significant cross agency review. There is a strong benefit to being at the Tier 1 level. There are two criteria for the Tier dichotomy – a risk informed dose limit and a quantity limit. The quantity limit for the Tier 1 launch is straightforward and shown in Table 9.

Table 9: Tier 1 Limits for Radioisotopes of Interest.

	Decay Energy	100,000 x A2 Limit	Tier 1 Power Limit
$^{60}\text{Co}$	2.6 MeV	$4 \times 10^4 \text{ TBq}$	16.7 kW
$^{238}\text{Pu}$	5.6 MeV	$1 \times 10^2 \text{ TBq}$	90 W

In addition to the material requirement, the risk-based dose requirements are also key for obtaining launch approval. The requirements are straightforward, but the task of showing how EmberCore technology can meet them is very complex. A complex probability risk assessment must be undertaken to evaluate launch failure probabilities. To approach this problem EmberCore employs a defense in depth strategy.

The EmberCore for the Extrasolar Express spacecraft is shown in Figure 18. The design of the system is focused on launch safety and safety for the ground crew integrating the spacecraft on a launch vehicle. The system is engineered with a defense in depth strategy with five robust layers with redundancy to prevent radioisotope release under any launch scenario (also see Figure 156).

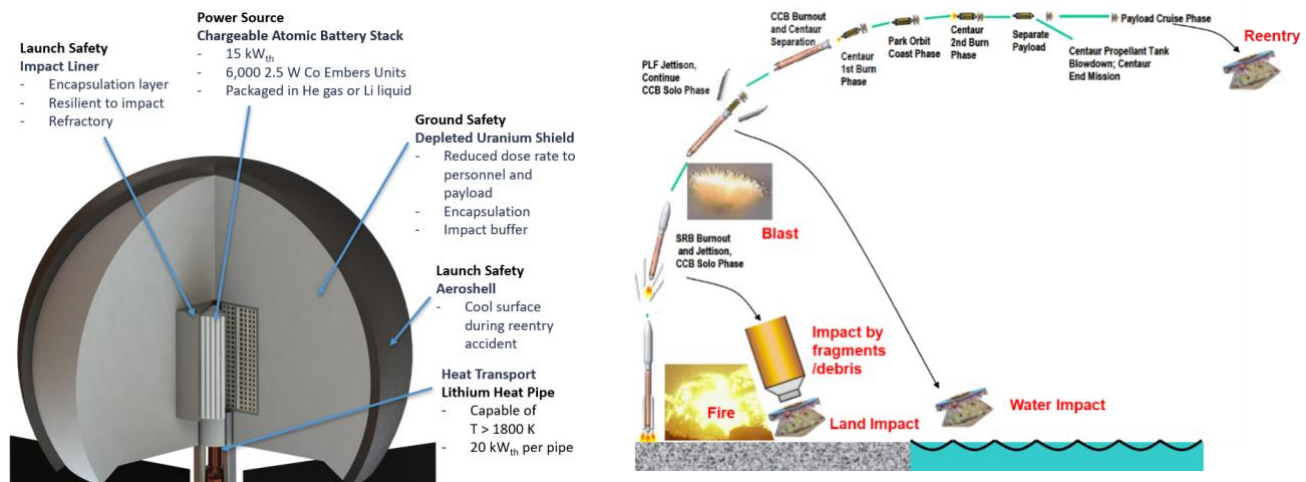


Figure 18: Left: 15 kW<sub>th</sub> ExtraSolar Express Mission EmberCore Design. Right: Launch Accident Scenarios<sup>12</sup>.



## Regulatory Qualification Mission

Significant time during the NIAC phase I has been dedicated towards preparing an EmberCore System for a Regulatory Qualification Mission (RQM) which can raise the Technology Readiness Level (TRL) and Regulatory Readiness Level (RRL) of the EmberCore technology as a whole by putting a low power thulia EmberCore in orbit with all necessary space and ground licenses. One of the most key components of the EmberCore from a licensing perspective is the Impact Housing/EmberBox, which will act both as the nuclear sealed source and a primary impact-absorbing layer. The EmberBox is expected to undergo a series of tests qualifying at as a nuclear sealed source in approximately April of 2022. Requirements it must meet are shown in the table below.

*Table 11: ANSI/HPS N43-6 Test Series Requirements.*

Temperature	Pressure	Impact	Vibration	Puncture	Temperature	Impact
-40°C (20 min), 600°C (1 h), shock 600°C to 20°C	7 MPa	200 g from 1 m	3 times 10 min, 500 Hz at 49 m/s <sup>2</sup>	50 g from 1 m	1000°C	Self-weight at terminal velocity

The first 5 requirements are the strictest possible requirements for an industrial radiography or ion generator source per ANSI/HPS N43.6. The final two requirements are estimated requirements to ensure an acceptable level of safety during the Preliminary Risk Assessment. We are still in the process of licensing specific launch codes from Sandia National Laboratories which will allow us to tune the FAA licensing requirements more finely, so for the time being, the final two requirements are treated as “soft” requirements. Although the EmberBox for a system with as many individual Embers as the Extrasolar Express would be larger than the EmberBox used for this RQM, the testing requirements would remain the same.

Preliminary material down-selection suggests that Inconel 625 is a good choice for the EmberBox material, per comparisons of the housing’s safety factor in direct and angled impact simulations, and of the dose rate at 30cm away from the EmberCore surface for equivalent EmberBox volume. Sample results of these simulations can be found below.

*Table 12: EmberBox Material Down-Selection Safety Factor Output.*

Material	Wall thickness(mm)	Total Mass(g)	Maximum Stress (Pa)	Safety Factor
Inconel 625	5.5	0.184749946	535711201	1.642676125
Inconel 625	3.5	0.103232146	558601370.4	1.575363124
Inconel 625	8.9	0.367181876	570777492.7	1.541756659
Stainless Steel 304	5.5	0.175069252	339558661.7	1.487224615
Stainless Steel 304	3.5	0.097822896	364840992.6	1.384164637
Stainless Steel 304	9.5	0.384404394	373848391.9	1.350814958
Aluminum/Silicon Bronze Alloy	5.5	0.17266205	478452419.3	1.254043194
Aluminum/Silicon Bronze Alloy	3.5	0.096477831	491098476.5	1.221750889
Aluminum/Silicon Bronze Alloy	9.5	0.379118833	510775813.3	1.174683657
Titanium Grade 36	5.5	0.124736842	517809905.6	1.05444101
Titanium Grade 36	3.5	0.069698813	543021264.2	1.005485486
R05255 Tantalum Alloy	5.5	0.369833795	579000069.5	1.001726996
Tungsten-Nickel-Iron-Cobalt Alloy	3.5	0.214598977	1313663042	1.001017733
Tungsten-Nickel-Iron-Cobalt Alloy	4.5	0.294713878	1322710798	0.994170458
Tungsten-Nickel-Iron-Cobalt Alloy	5.5	0.384058172	1328047108	0.990175719
Titanium Grade 36	2.5	0.046518788	554175735	0.985247035
R05255 Tantalum-Tungsten Alloy	3.5	0.206650867	593410297.9	0.977401306
R05255 Tantalum Alloy	6.5	0.465216111	595007779.1	0.974777172

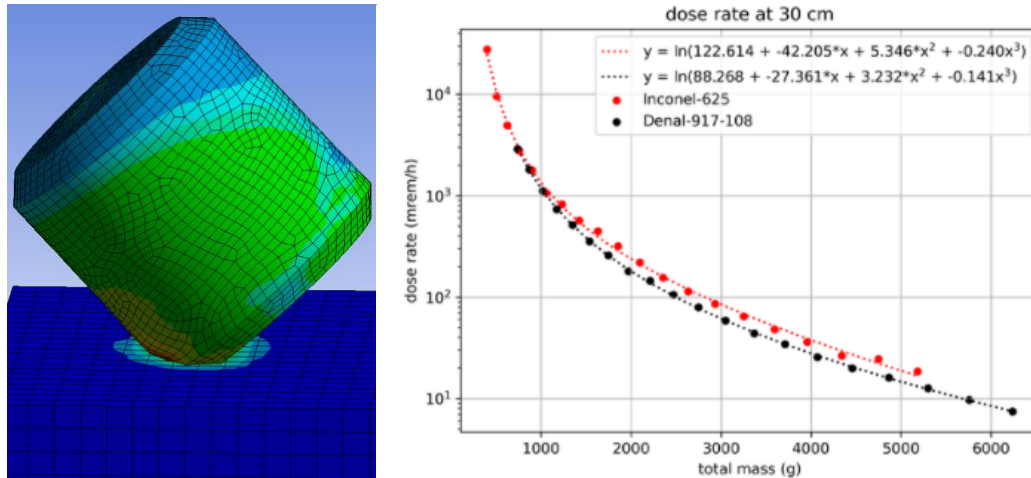


Figure 19: EmberBox safety factor and dose rate simulations.

Following this preliminary material down-selection, a series of simulations was carried out to ensure that the EmberBox, as currently designed, can survive the NRC Sealed Source test series. Pressure, impact, and puncture simulations were focused on, estimated as a static equivalent load. Sample results from these simulations can be seen below, none of which predict the Inconel 625 reaching its ultimate strength, even at high temperature.

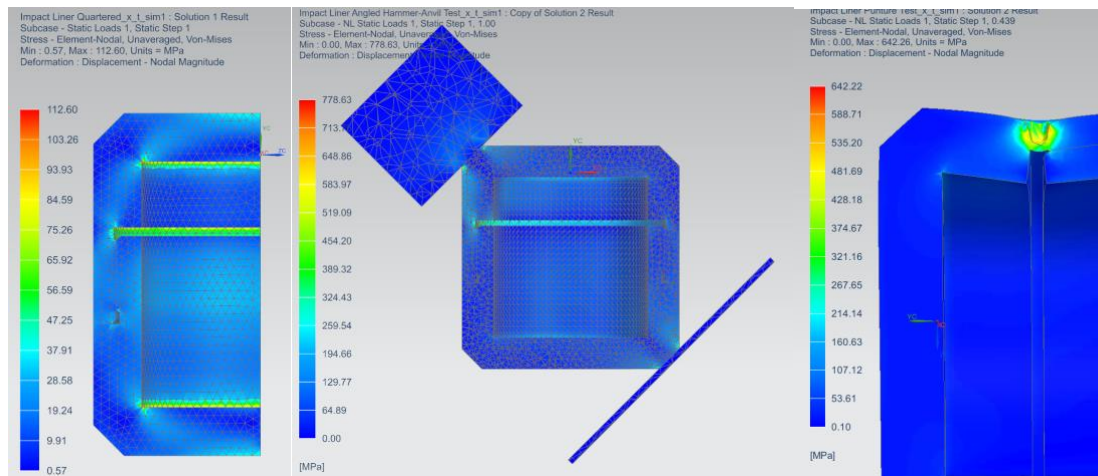


Figure 20: Pressure, impact, and puncture simulation results, respectively.

Another important component of the EmberCore RQM that was investigated during the NIAC Phase I was the impact cushion, which sits between the EmberBox and the individual Embers, ensuring that they do not break in the event of an impact scenario. Preliminarily, we plan to have a compressible substance at a thickness equivalent to .75x the maximum deformation of the EmberBox in simulations, on both sides of the EmberStack. This allows all deformation to be absorbed by the cushion as it compresses to approximately 1/3 of its size.

To ensure manufacturability in a hot cell environment, required for both the RQM and eventual assembly for the Extrasolar Express EmberCore subsystem, we approximated the EmberBox as a steel tube and utilized

various densities of partially rigidized ceramic wool to achieve an easily hot-cell-sealable configuration. An approximated manufacturable cushion configuration can be seen in the image below.



*Figure 21: EmberCore Impact Cushion.*

Though these subsystems are not directly a part of the Extrasolar Express Spacecraft, this preliminary RQM will be critical for raising the TRL and RRL of the EmberCore technology, for additional cobalt-based RQMs and thulia-based EmberCore missions in the near future, and eventually for cobalt-based EmberCore spacecraft missions.

## 5. Extrasolar Express Spacecraft

While raising the TRL and regulatory readiness of the EmberCore technology has been a central focus of the work done in Phase I, work has also been done on the design of the spacecraft itself. The spacecraft is conceptualized as an extremely small system, with a total height of 3 m along its longest axis and a wet mass of only 1200 kg. A mass breakdown and size comparison are shown in Table 8. As designed, the craft uses a Cobalt-60 EmberCore thermal power source, lithium heat pipes, and high-efficiency thermoelectric generators to supply power to an electric propulsion system. In this way, the spacecraft leverages the high specific impulse of electric propulsion without dependence on the sun, the strength of the EmberCore technology. The overall power balance as thermal power is converted radiated and converted to electrical power, and finally distributed to all spacecraft systems, is shown below. Individual subsystems will be further detailed.

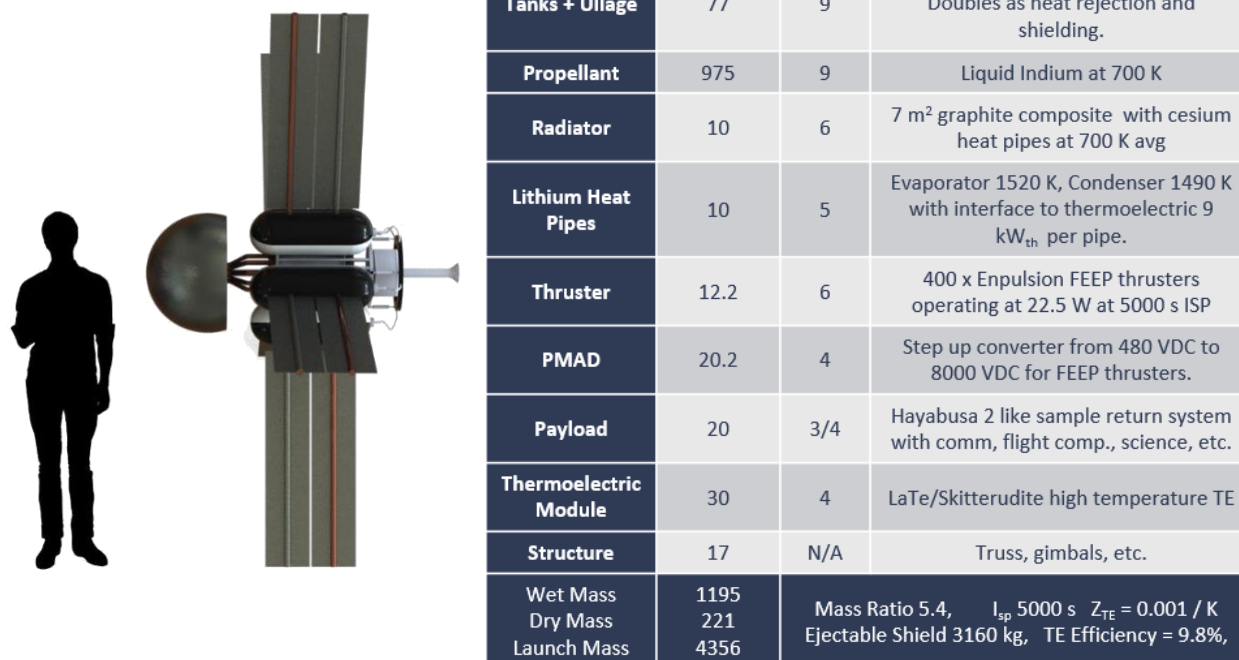


Figure 22: Left Extrasolar Express Spacecraft, Right the Spacecraft Mass Budget. Power System Specific Mass of 7.65 kg/kW<sub>e</sub>

A power balance which was informed by a basic thermal and electric network analysis is shown in Figure 23. Using the same assumptions as in Figure 22, but with a variable payload and variable I<sub>sp</sub>, a contour plot of the ΔV performance of the Extrasolar Express spacecraft is shown in Figure 24. Two different thermal power levels are shown to demonstrate how the technology can be scaled down. A 1 kW<sub>th</sub>, 10 kW<sub>th</sub>, and 100 kW<sub>th</sub> system could complete a flyby, rendezvous, and sample return respectively with a 20 kg payload.

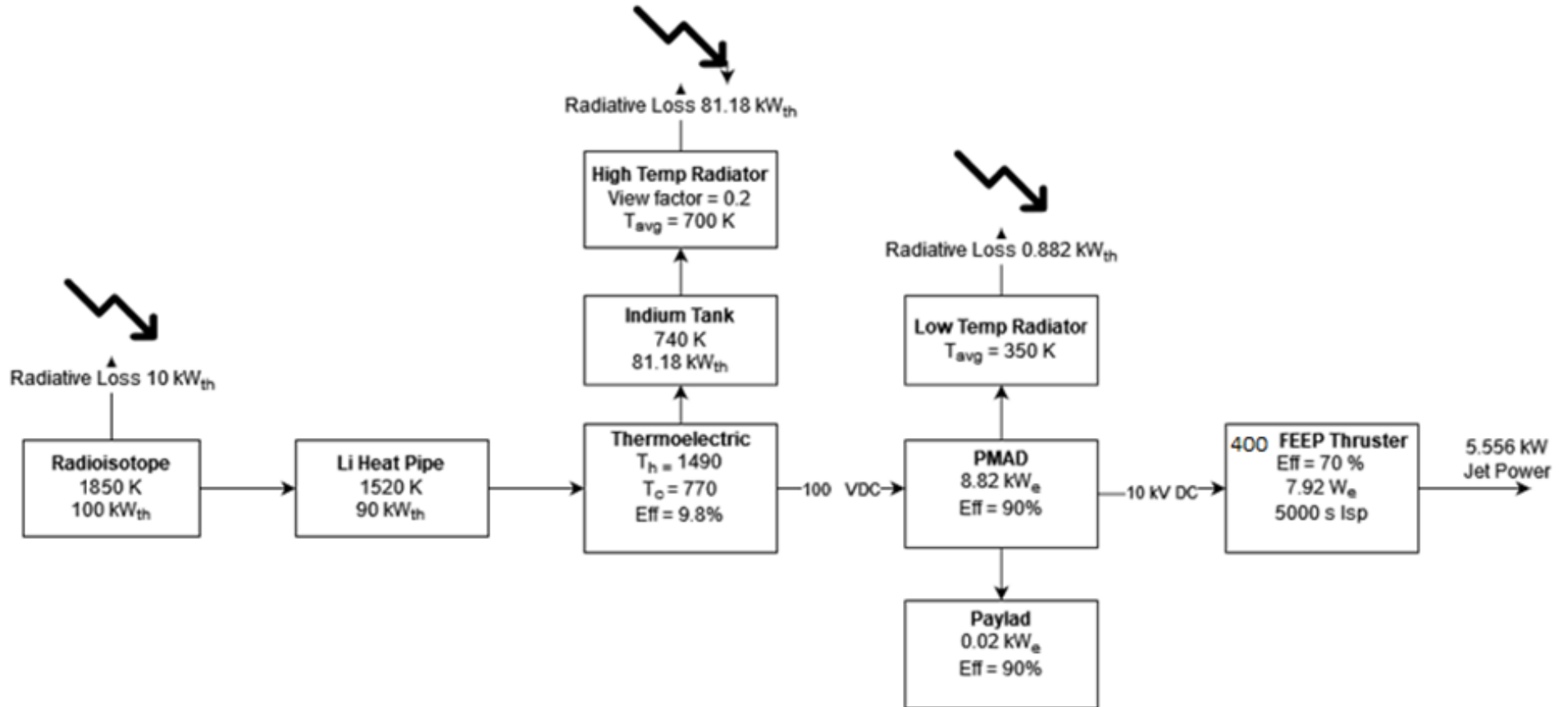


Figure 23: Power Balance

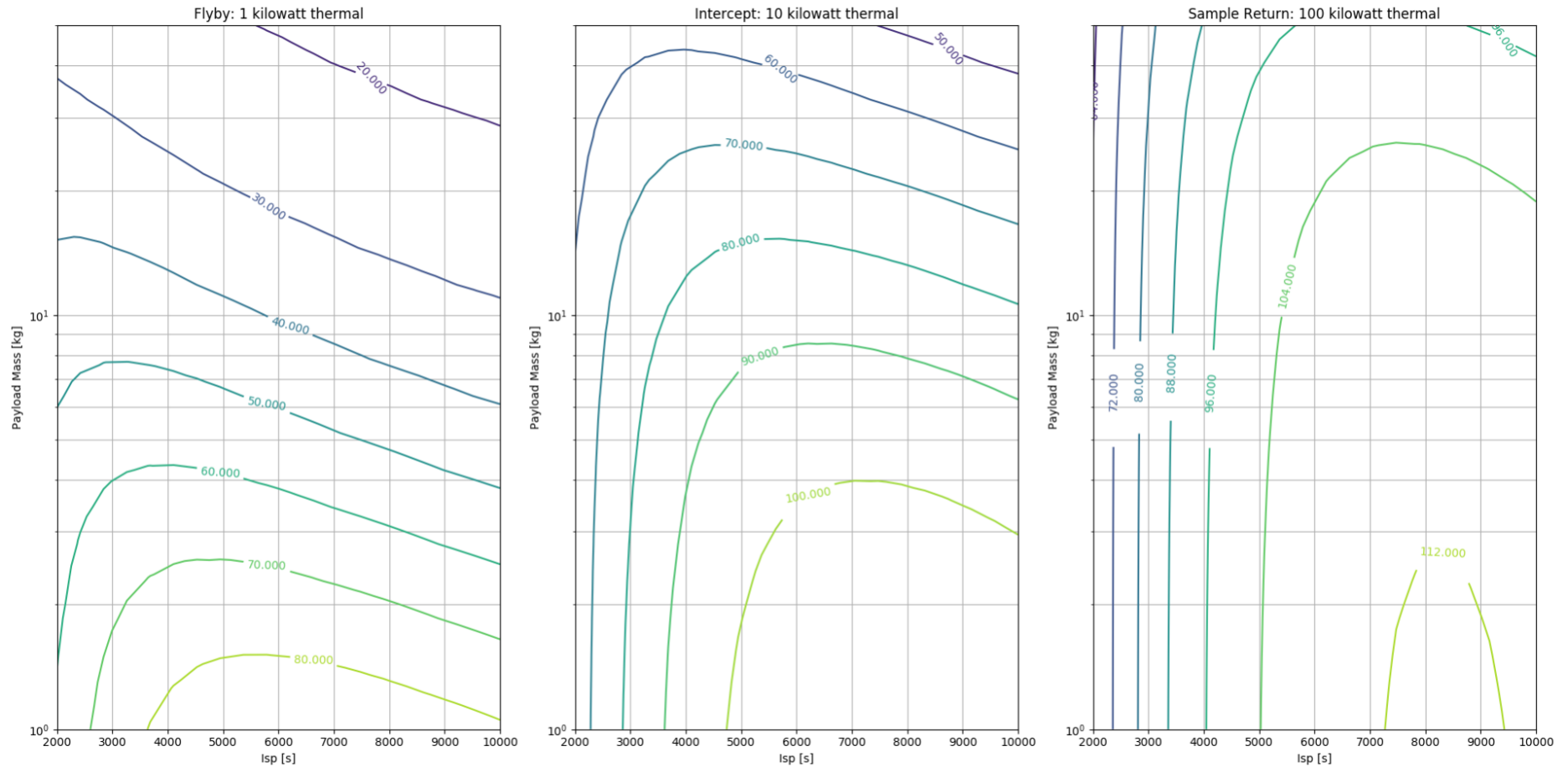


Figure 24: Delta-V Contour Plot of the Extrasolar Express with three Different Thermal Power Levels.



The payload mass is a major determinate of the total  $\Delta V$ . If the sample return payload can be miniaturized, then even the 1 kW<sub>th</sub> could complete a sample return mission.

A conceptual render of the Extrasolar Express with a 100 kW<sub>th</sub> EmberCore, an appropriate mass of indium propellant, and a conceptual payload for a sample return mission is shown in Figure 25 below. This conceptual design will be further explored in the following sections

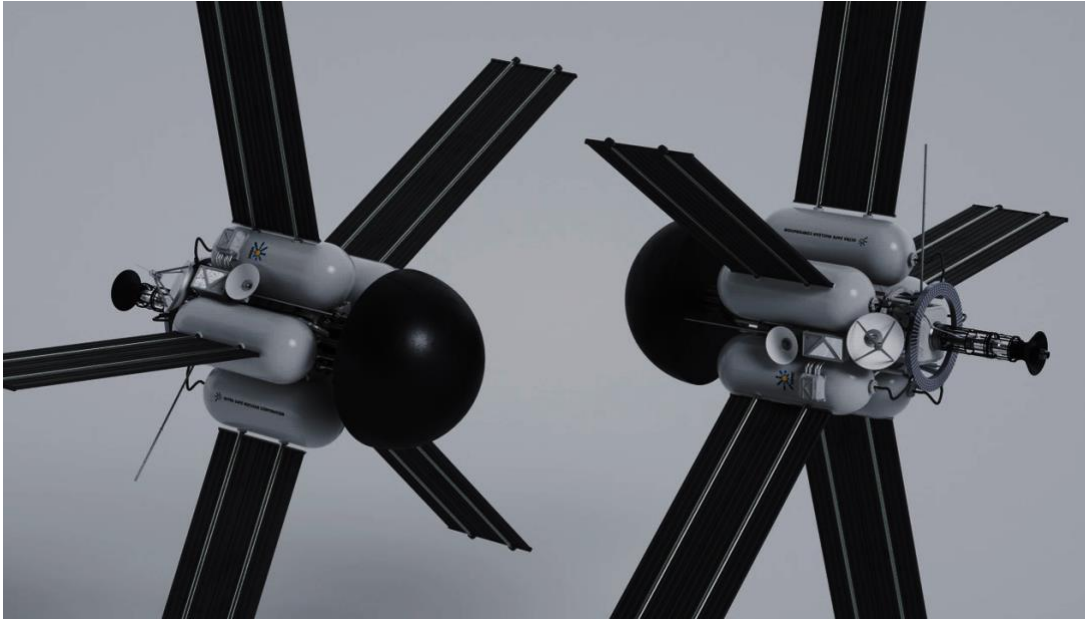


Figure 25: 100 kW<sub>th</sub> Extrasolar Express

## Spacecraft Subsystems

The spacecraft can be divided into several subsystems which interface with each other but continue to function mostly independently of each other. The subsystems explored during this design phase were the EmberCore, High Temperature Power Conversion, Thermal Waste Management, Electric Propulsion, Core Structure, Radiation Dose Management, and Sample Return. These subsystems will be further fleshed out and analyzed during the NIAC Phase II, and additional subsystems including controls and communication will be explored.

Cobalt-60 and Eu-152 are both strong gamma emitters. Traditionally atomic batteries have been alpha or low energy beta emitters that produced little x-ray radiation. Cobalt-60 has two strong characteristic x-rays at energies close to 1 MeV. Shielding 1 MeV x-rays to levels tolerable to electronics and humans is very mass intensive. A depleted Uranium four pi shield was designed in the Phase I with a mass of

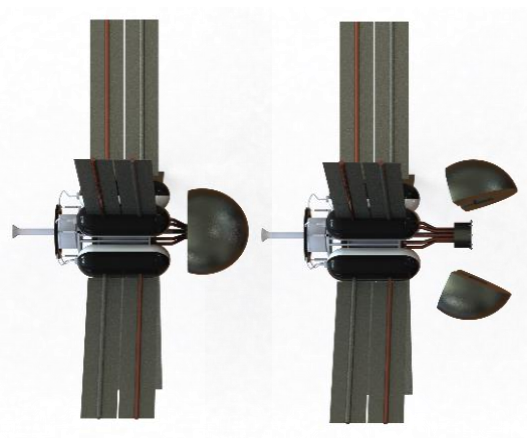


Figure 26: Shield Ejection Process

3160 kg which protected ground crew assembling the spacecraft to less than 2 mrem/hour one meter from the surface.

Once launched into a nuclear safe orbit (900 km or higher) the shield and accompanying aeroshell are not required. They are ejected in orbit leaving only a small shadow shield to protect the electronics of the spacecraft (which are radiation tolerant compared to ground crews).

The components of the power conversion system are resilient against radiation effects. Heat pipes are unaffected by x-rays and the solid-state power conversion modules (thermoelectric or thermionic) are highly resilient against radiation.

The voltages from the solid-state converters are then routed to a PMAD device which steps up the DC voltage for the FEEP thrusters. The PMAD device and the spacecraft computer are the most sensitive components on the spacecraft and can utilize directional spot shielding.

The Indium propellant tanks also act as a shield. The tanks are low pressure, high density and thin walled – the perfect combination for shielding. As the tanks empty, they are ejected, however because there are multiple tanks, they can be ejected intelligently to maintain proper spot shielding.

In addition, an optional extendible boom can be added to increase the distance between the sensitive components and the EmberCore. This combination of shielding strategies is analyzed in the Phase I final report and found to be effective.

### High Temperature Power Conversion

A key element of EmberCore is its ability to produce high temperature heat. High temperature heat is beneficial for compact power conversion devices. The higher temperatures allow for higher efficiencies and allow for heat rejection at higher temperature which greatly minimizes the spacecraft mass. TRL 5

Thermoelectric power conversion using LaTe/Skutterudite thermoelectric were baselined in the Phase I study. These could obtain an estimated 8-11 percent conversion efficiency. Higher TRL but lower efficiency SiGe would be able to obtain 6-8 percent efficiency. The study results are shown in Figure 28. The results show a straightforward path for development with the LaTe/Skutterudite based power system able to obtain a specific mass under 8 kg/kW<sub>e</sub> and the SiGe obtaining closer to 12 kg/kW<sub>e</sub>. One key research area is the ability of these traditional thermoelectric to withstand the intense gamma ray radiation. Generally, the performance would be unaffected as the semiconductor materials are being used for bulk properties, as opposed to integrated circuits that rely on microscopic properties.



*Figure 27: Extrasolar Spacecraft with Ejected Tanks*

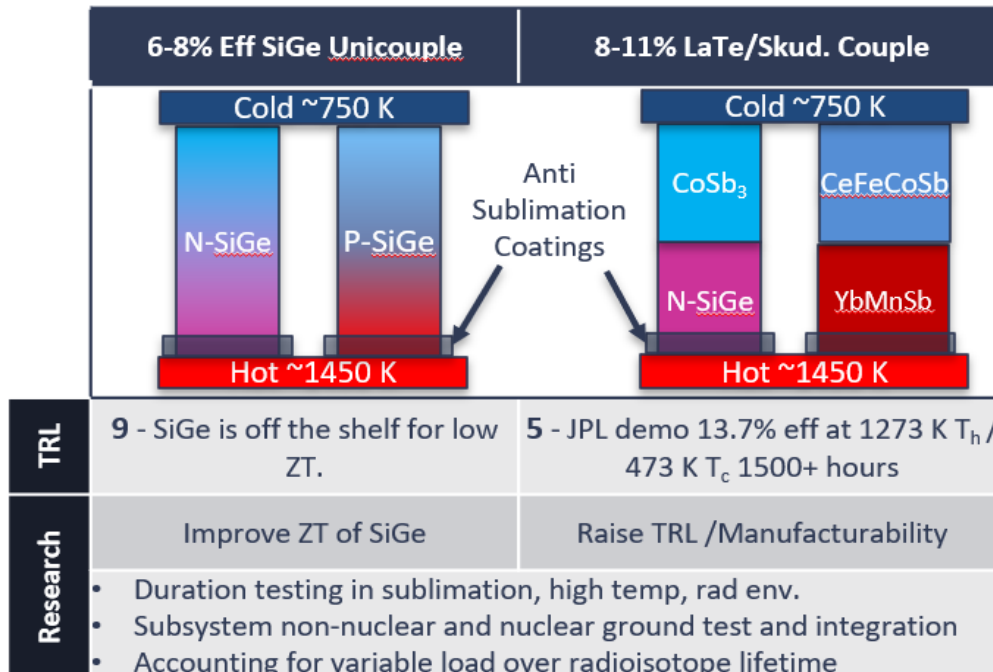


Figure 2819: Thermoelectric Power Conversion Options.

There are other power conversion options that are very promising. Specifically, the ATEG from Howe Industries (and the subject of a Phase II NIAC study itself), the NTAC under development at NASA Langley, and the thermionic power conversion technology from Modern Electron. These devices generally promise an efficiency closer to 20 percent which would enable power conversion system with a specific mass closer to 4 – 6 kg/kW<sub>e</sub>.

## Electric Propulsion

High specific impulse will be achieved through use of a Field-Emission Electric Propulsion (FEEP) system. This enables us to take advantage of the high  $I_{sp}$  of electric propulsion, utilizing the electrical power output of the EmberCore System and the High Temperature Power Conversion system to remove dependence on solar power. Use of FEEP enables use of liquid metal propellant, allowing us to volumetrically shrink the spacecraft and remove pressurization requirements for the propellant tanks. FEEP Thrusters are a high-TRL system, having been previously demonstrated in-orbit as CubeSat propulsion. Though no manufacturer partnerships have been established, nominal values of  $I_{sp}$ , power requirements, and thruster array size requirements are drawn from specifications of Enpulsion's Micro R<sup>3</sup> and Nano R<sup>3</sup>. Indium was chosen as an effective propellant for the thrusters due to its high atomic weight and relatively low melting point. As individual FEEP thrusters are very small and provide little thrust, a large array of FEEP thrusters is required to propel the Extrasolar Express. As currently designed, the thrusters will be mounted in a ring around the Sample Collection

subsystem, on a gimbal mechanism which would allow for directional thrust. The baseline mechanical design of the thruster array can be seen in Figure 292029.

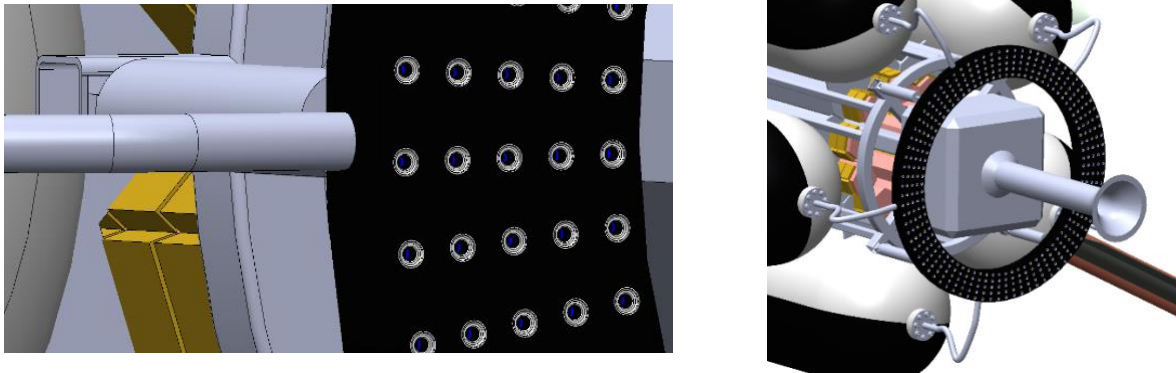


Figure 2920: FEEP Thruster Array

Per Enpulsion's indium thruster specifications, an  $I_{sp}$  of up to 6,000 s is possible with state-of-the-art FEEP thrusters. The Micro R<sup>3</sup> thruster array consists of four indium FEEP thrusters and consumes a total of 100W, including power consumed for propellant heating and neutralization. As the Micro R<sup>3</sup> consumes less power than four Nano R<sup>3</sup>s, we can see some increase in power efficiency with increased array size. In addition, we will be heating our propellant externally to the thruster array. From these observations, we can estimate a conservative 22.5 W<sub>e</sub> consumed per FEEP thruster. From our total electric power supplied of approximately 9 kW, we can calculate a baseline thruster array size of 400 thrusters.

### Thermal Management

Thermal power is transported from the EmberCore system to the High Temperature Power Conversion system by ten lithium heat pipes, each capable of removing 9 kW<sub>th</sub> from the EmberCore with evaporator and condenser temperatures of  $T_e = 1550$  K and  $T_c = 1490$  K, respectively. These temperatures were determined via preliminary analysis of the thermal power output of the EmberCore system. Overall properties of heat pipes were estimated from SP-100 data.

The thermoelectric power conversion system has an efficiency between 6% and 20%. To maintain a conservative estimate of waste heat generated, while still accounting for higher efficiency thermoelectric power conversion that is possible, we estimate a power conversion efficiency of approximately 10%. This leaves approximately 81 kW<sub>th</sub> waste heat to be rejected. Choice of approximate power conversion efficiency was also informed by SP-100 data.

To improve the overall power efficiency of the system, rather than electrically heat metal propellant, as is typical of FEEP thrusters, we heat the propellant using waste heat from the power conversion system before radiating it. This can be seen in Figure 23, power balance. To accomplish this, the spacecraft contains conductive pathways between the cold end of the thermoelectric generators ( $T_c = 770$  K) and the propellant tanks. This is shown for the 5 standard vessel and the 10 annular vessel orientation in Figure 302130.

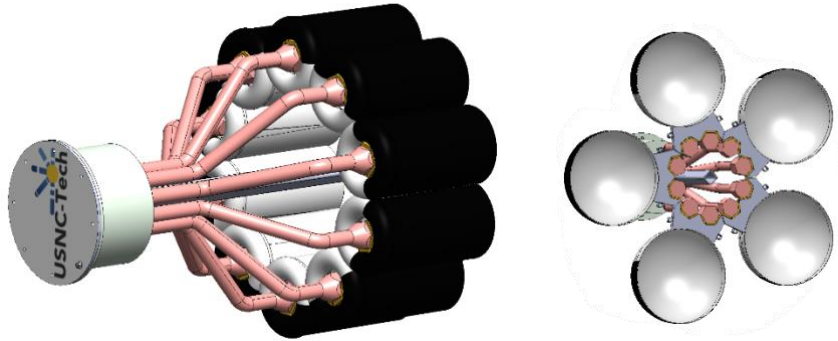


*Figure 3021: EmberCore Heat Pipe Arrangement and Propellant Heating Pathways*

The melting temperature of Indium, our chosen liquid metal propellant for the FEEP system, is 157°C. As a section of the tank will be held to a fixed temperature of 770 K, once the system reaches steady-state, the majority of the Indium will be heated to well above its melting point.

Past the thermal conduction pathway through the propellant tanks, the 81 kW<sub>th</sub> must be radiated to the environment. This is done using cesium heat pipes connected to the Indium tanks and graphite composite radiator fins. In addition, some heat will be radiated through the bodies of the propellant tanks themselves. The outer part of the tanks will be coated with a high-emissivity material, while the inner part of the tanks will be coated with a low emissivity material. This is done to avoid reradiating heat to other tanks and to structural trusses.

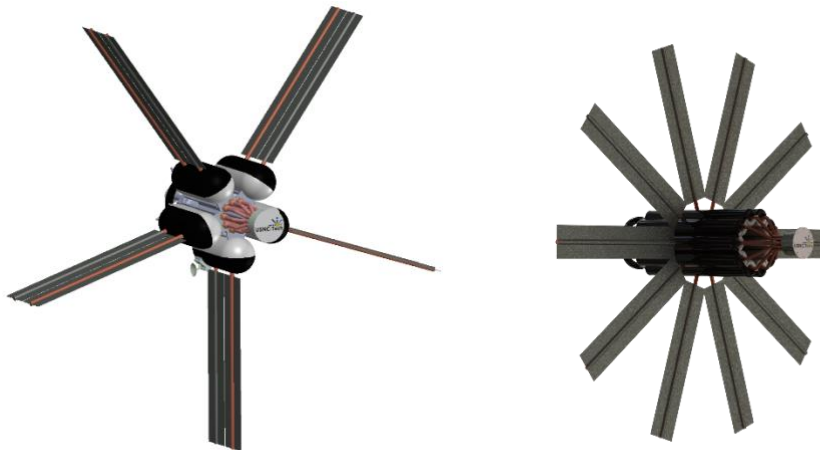


*Figure 3122: Radiator sizing and orientation on 5-tank and 10-tank arrangement crafts*

Assuming an average radiator temperature of 700 K based on preliminary thermal analysis of radiative loss ratio between the fins and tanks, a fin emissivity near 1, and a radiative view factor adjustment of 1.2 in a five-tank arrangement, a radiator panel size requirement of 7.15 m<sup>2</sup> was calculated. The same calculation yields a 5.95 m<sup>2</sup> radiator panel requirement in a ten-tank arrangement. These radiator panels, appropriately



sized, are shown in the mechanical baseline model in Figure 312231. If a detachable propellant tank design is pursued, further work must be done in sizing the radiators – however, we anticipate that the sizing will not change significantly, due to the increases in temperature in the remaining radiator panels.

To account for any inefficiencies in the payload and PMAD systems, a low-temperature radiator is required at the payload end of the spacecraft. These radiator panels would have to reject approximately  $.89 \text{ kW}_{\text{th}}$ , and assuming an average panel temperature of 350 K, would be approximately  $1 \text{ m}^2$ . These panels would be connected to all components generating heat they cannot reject on their own and would be attached to the payload end of the craft in a boom deployment scenario.

Some thermal loss is expected from the unshielded EmberCore system at the front end of the craft. Based on its thermal output and surface area, we anticipate a radiation thermal power loss of approximately 10 kW.

### Structure

There are two proposed arrangements of propellant tanks. As we require ten heat pipes to carry all thermal power output from the EmberCore system to the TEGs, most cyclically symmetric options are 5 or 10 propellant tanks. The propellant tanks must each be heated using waste heat on the cold side of the thermoelectric modules, to ensure that the Indium remains liquid during thruster operation. The 5-tank structure is conceptualized as using standard-shaped Inconel pressure vessels with hemispherical heads, sized appropriately to handle the hydrostatic loads of liquid indium and the vapor pressure generated at 700 K. Maximum loads in the tank walls are taken from ASME code case for low-temperature long-duration operation of an Inconel 617 pressure vessel. The tanks have walls approximately  $1/16''$  thick. The 10-tank configuration consists of annular pressure vessels, one around each pressure vessel/TEG assembly. The two tank configuration concepts can be seen below.

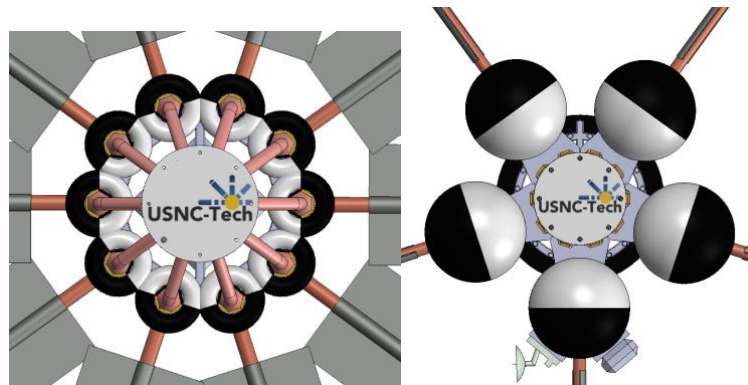


*Figure 3223: Tank Sizing and Orientation on 5- and 10-tank configurations.*

Each configuration has pros and cons. The primary pro of the 5-tank system is reduced mass compared to the 10-tank system, due to the lower number of tank walls and relatively small size of the thermal pathways compared to the necessary size of the tank walls. In addition, the 10-tank system requires an increase in the overall volume of the craft in the radial and axial directions, due to the constraints of adding an annular tank with non-negligible volume around each of the heat pipes.

The 5-tank configuration would, with further design effort, be capable of ejecting emptied tanks during operation, as shown in the graphic below.



This enables further increases in  $\Delta V$  as the craft continues along its trajectory, further decreasing the mass of the system. Center of mass balance would need to be achieved via control of propellant level in remaining tanks. Tanks would be connected to both the electric propulsion system and thermal pathways via a set of



*Figure 3324: Extrasolar Express with Ejected Tanks.*

TiNi Frangibolt Actuator-equipped fasteners, allowing for non-pyrotechnic fastener release. The pressure vessels can then drift free from the craft.

The primary pro of the 10-tank configuration is uniformity across the tanks in terms of heating, heat flow, and radiation. In addition, the 10-tank configuration allows a radiator panel configuration that prevents and efficiency loss from radiative view factor, slightly reducing overall radius of the craft.

Overall, we do not expect the pros of the 10-tank configuration to outweigh the mass penalty it incurs. To this end, we have chosen to select the 5-tank configuration as a baseline.

Structural beams along the main axis of the craft and against the propellant tank support structure work to hold the Sample Return, EmberCore, and Power Conversion subsystems together. This structural support structure, beneath the pressure vessels, can be seen below. Conceptually, this structure will be made from .75" and .5" square steel tube, welded together. Detailed structural analysis of the support structure will be conducted during phase II.

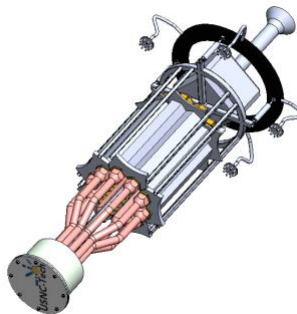


*Figure 3425: Extrasolar Express Core Structure.*

## Radiation Dose Management

On the ground and during launch on the baseline Falcon 9, the full radial shield assembly remains attached to the EmberCore System, as shown in Figure 25. We used software, Attila4MC, for high-fidelity radiation shield modeling of the 5-tank spacecraft. With Attila4MC, the CAD geometry was imported into a MCNP 6.2 model using an unstructured mesh of tetrahedral cells. Using this mesh, Attila4MC enables powerful variance reduction techniques (CADIS and FW-CADIS) to accelerate Monte Carlo radiation transport calculations, which is crucial for the spacecraft where more than 10 orders of magnitude of attenuation is expected for the Depleted Uranium shield (i.e., <1 out of 1 billion source gamma rays penetrate the shield). The Consistent Adjoint Driven Importance Sampling (CADIS) technique generates optimized weight windows from an Attila adjoint calculation, including with energy source biasing, which is ideal for deep penetration cases where the solution is desired at or around a single detector. Forward-Weighted CADIS (FW-CADIS) generates weight windows that are optimized for multiple detectors, large regions, or the entire computational domain. It is ideal for visualizing the MCNP solution everywhere.

To demonstrate this high-fidelity modeling capability and assess the radiation shielding design, FW-CADIS was applied on a simplified CAD model of the 5-tank spacecraft with a Co-60 source (1.17 MeV and 1.33 MeV gamma rays). Figure 35 shows contour and iso-surface plots of dose response (rem/h per Co-60 decay). It should be noted that the heat pipe and tanks were empty in these models and will be added in later modeling efforts.

Future work using this modeling capability includes evaluating:

1. scaling of dose rates to account for Co-60 activity at a given power level;
2. local radiation heating in all spacecraft components; and
3. evaluating total ionizing dose (TID) in electronics over the mission lifetime.

Based on these results, shielding may need to be redesigned and/or the spacecraft may need to be reconfigured to meet radiation protection requirements.

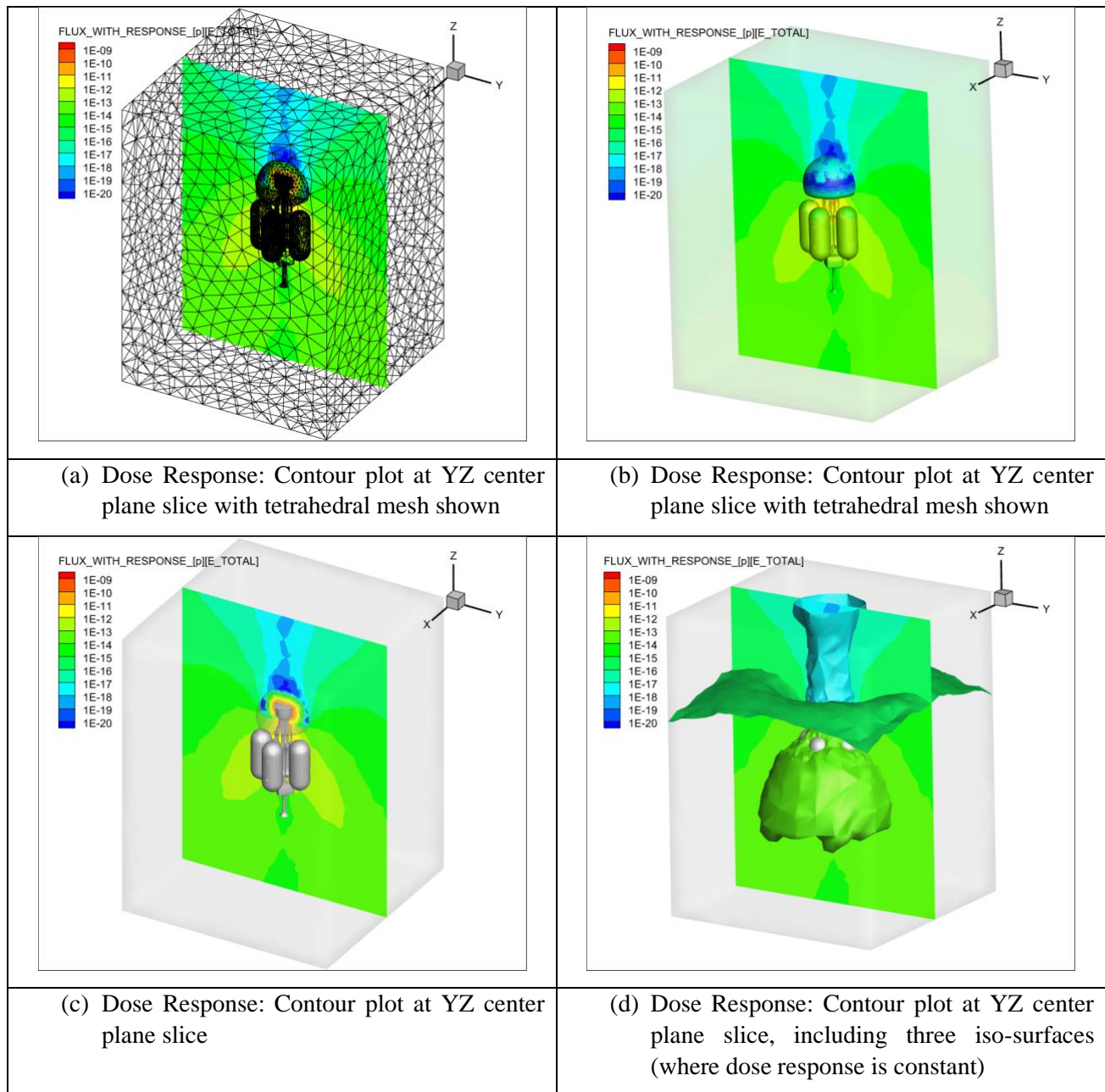


Figure 35: MCNP 6.2 Model Results Using Attila4MC

Once in orbit, the Extrasolar Express will detach the primary shield, which will split into multiple pieces. These pieces will be detached from each other using pyrotechnic fasteners. If necessary, actuators to give the pieces of the primary shield momentum away from the spacecraft body will be added during the second design phase. A mock-up of this process can be found in Figure 26.

The shadow shield will not be detached along with the primary shield. The shadow shield is not modelled in the current mechanical baseline model, as preliminary sizing to meet component dose rate tolerance has not yet been conducted. Detailed design on the shadow shield will be performed during phase II.

A concept that has not yet been explored in much detail is the idea of adding a collapsing slit-tube boom along the central structural axis. As radiation dose decreases with the square of distance, increasing the distance between vital electronic systems and the EmberCore system could be key to keeping systems below their allowable dose rate. As long as thrust is primarily along the central axis of the boom arm, it should not be required to undergo a large stress load. Necessity of this system will be established as Atilla4MC simulations are completed, and structural analysis will be completed as a supplier is established.

### Sample Return Payload

The primary payload of the craft is currently extremely notional. The idea behind the system is to function similarly to the sample return payload of the Hayabusa spacecraft. As such, in the baseline mechanical design model, the system is roughly based on this payload. A greater understanding of the payload and its needs would help inform whether to pursue the 100 kW<sub>th</sub> spacecraft or the 15 kW<sub>th</sub> spacecraft for the future.

### Mission Conops

The spacecraft will launch from Earth on a Falcon 9. Because of its low mass, the Falcon 9 can provide a large  $\Delta V$  boost with a  $C3 > 10 \text{ km}^2/\text{s}^2$ . The spacecraft then travels toward a planet such as Jupiter or Venus to perform a place change maneuver and accelerates towards the Extrasolar Object. After accelerating towards the object for some distance the spacecraft flips around to begin deceleration. Once near the object the spacecraft will match speed and collect a sample in a way like the Hayabusa II<sup>11</sup> or the Deep Impact<sup>12</sup> missions. The spacecraft will plot a return trajectory. As it nears Earth it will eject the samples in a container which aerobrakes and lands on Earth. The spacecraft will travel away from Earth to limit the chance of re-entry. After a period of 10 half-lives (approximately 50 years) the radioactivity will diminish to a point to where it no longer poses a radiological hazard.

## 6. Phase II and Phase III Technology Maturation Plan

We will build upon the results of the Phase I and move towards a raising TRL, regulatory readiness level and ultimately towards a credible path to flight. The plan is described in Table 13.

*Table 13: NIAC Phase II and Phase III Technology Maturation Plan*

	Phase II (2022-2024)	Phase III (2024 -2026)
<b>Regulatory Qualification Mission</b> Raise RRL	-FAA preapplication for payload approval for a low power but regulatorily relevant Cobalt EmberCore. -Relevant NRC/DOT licensing to support the regulatory qualification mission. -Talks with launch partners	-Fly a low power, but regulatory relevant EmberCore to space to demonstrate regulatory readiness level. -Full power ground demonstration licensing support
<b>Ember Irradiation Campaign</b> Raise Ember TRL	-Manufacture irradiation ready embers -Low power irradiation (ember TRL 2 -> 4)	-Demonstrate full power ember (TRL 4->6) -Produce > 100 W of embers to demonstrate supply chain
<b>Power Module Design</b>	-Conceptual designs with partners	-Power conversion demo with partners

<b>Power System TRL</b>	-Decay power reduction analysis	
<b>Spacecraft Design</b> Spacecraft TRL	-Refine spacecraft conceptual design. -Select between 100 kW <sub>th</sub> or 15 kW <sub>th</sub> -Develop payload conceptual design.	-Identify suppliers and component qualification pathways
<b>Trajectory</b> Mission Analysis	-Continuous thrust modeling -Larger Sample of Extrasolar Objects -'Oumuamua Intercept Mission	- Select Mission Plan - Work with professional mission planner

During a future NIAC Phase II, the spacecraft subsystem designs proposed will be further matured, from baseline conceptual designs into preliminary designs. Revisions will take place to ensure that each subsystem functions as intended and interfaces seamlessly with other subsystems, and reviews will be conducted to ensure that each component is at an acceptable level of design thoroughness. In addition, subsystems that have not been conceptualized during phase I, such as communication and control systems, will undergo design during phase II. A more in-depth thermal analysis, detailed gamma ray dose for each component, detailed conops, and ground integration. The sample return payload will also go through more scrutiny as well to see if it can be miniaturized and if so, the baseline spacecraft may be reduced in power to 15 kW<sub>th</sub> reducing the size of the spacecraft while maintaining the 100 km/s capabilities. A team member with a strong background in spacecraft design will be brought in and effort will be dedicated to reaching out to scientists to better determine what should be in the payload (in addition to a sample return device).

During a future Phase II and Phase III NIAC regulatory progress would continue to be made and focused toward a low-power simple flight demonstration to raise the technology readiness level. Phase II will work toward licensing the launch and a Phase III would see a flight demonstration will launch a small but regulatorily relevant amount of Co-60 into space (no power conversion). The Co-60 would take the form of a mW or  $\mu$ W scale ember(s). At lower power, these embers will be produced in a low power research reactor. Significant engineering work will be put into packaging into the proper safety systems (aeroshell, shield, housing, etc.). USNC-Tech will work heavily with NRC, FAA, and other regulatory agencies on the regulatory demonstration implementing the guidelines set forth by NPSM-20 under a Tier 1 launch license. launched into a 50 year or greater to allow for sufficient decay. While reduced in scope, this low-power launch lays the foundation for future higher power launches and would be the first commercial launch of nuclear material into space.

The Phase II and Phase III NIAC will enable a full-power ground demonstration of Cobalt embers. In Phase II the ember materials will be matured, and a low power ember would be produced with reactor partners and in Phase III the full power embers (on the order of a few watts per ember) will be produced with a high flux reactor partner. We believe that a TRL 6 ember with at least a power density of 4 W/cm<sup>3</sup> be achieved by the end of a Phase III.

The trajectory work will be further refined with additional team members with strong orbital mechanics qualifications and evaluate more mission scenarios for extrasolar objects including some analysis of a possible 'Oumuamua intercept mission launched in the late 2020s.

Power conversion for this Phase I was mostly a literature review, however many conversations were had with key partners and a Phase II includes bringing on power conversion partners. Currently the high TRL JPL high temperature thermoelectric technology is baselined, however some possible partners can bring higher

performance and higher temperature systems which can further improve the performance of the spacecraft. A Phase II will inform a technology selection and a Phase III would involve ground demonstration of the power conversion system.

## 7. Conclusion

This NIAC Phase I study has taken a closer look at the EmberCore powered radioisotope electric propulsion technology and in the process matured the concept, matured the regulatory pathway, and even resulting in the development of some early state ember prototypes. The conclusions have been put into a bulleted list below.

### Raised TRL of Cobalt EmberCore radioisotope technology from 1 -> 2

- **Modelling:** Analyzed target design and retired risk from self-shielding and encapsulation material degradation in irradiation
- **Target Manufacture:** Prototype Cobalt and Europium embers manufactured in our lab
- **Charging:** Established relationship with irradiation partners and established credible pathway for 10-100 kW production using existing facilities
- **Maturation Plan:** Strategy developed for irradiation campaign toward TRL 6 ground demonstration by the end of a Phase III NIAC

### Raised Regulatory Readiness Level (RRL)

- **Engagement with NRC:** Have a 10 CFR Part 30 possession license and a sealed source license. These licenses enable USNC-Tech to handle radioisotope material for future phases.
- **Pre-Application Engagement with FAA:** Officially engaged with the FAA under the guidance of NPSM-20.
  - Established concept of a Tier 1 regulatory qualification mission to raise RRL
  - Determined with the FAA that the qualification mission falls under a 10 CFR 450 partial payload approval
  - Established line of jurisdiction between the NRC and FAA in launch and launch integration.
  - First of a kind licensing process is not well defined. Still significant unknowns to obtain a launch license, but a general strategy has been formulated and introduced to regulators.

### Established Notional Spacecraft Design

- **Power Conversion:** 5-8 kg/kW<sub>e</sub> power system is achieved with high temp. rad-hard solid state power conv. Baseline design using LaTe/Skudderidite at 1450 K T<sub>h</sub>. SiGe high TRL, lower performance also studied. Thermionic and advanced thermoelectric enable < 5 kg/kW<sub>e</sub>.
- **Spacecraft:** COTS FEPP liquid metal thrusters found to achieve I<sub>sp</sub> needs. The liquid metal tanks are synergistic with radiation protection and thermal management. Ejectable shield and tanks

### Mission

- **Trajectory Analysis:** Using GMAT simulation the Extrasolar Express architecture indeed enables sample return on 10–15-year timelines

### Key Takeaways

- A 2030 flight of the Extrasolar Express or at least a lower capability (>50 km/s) prototype is credible
- Key challenges to flight are regulatory/launch approval. Technological challenges exist for achieving highest level of performance (> 100 km/s), but lower levels of performance (>50 km/s) are low risk
- The radioisotope electric propulsion architecture is scalable to very small packages - scaling down to a 1-3 kW<sub>e</sub> system reduces regulatory risk by decreasing from a Tier 2 to a Tier 1 launch Acknowledgements



- This \$125,000 Phase I NIAC has demonstrated a credible path forward and we would like to continue development

## 8. Acknowledgements

Thank you to the NIAC program. I have been inspired by the NIAC program since my college days and this Phase I NIAC was the seventh proposal I as the PI have submitted. It is an honor to be a NIAC fellow. While the NIAC is not quite to the level of the Nobel Prize, to me personally it is a close second. When I chose to pursue my Ph.D., it was because I had an incredible desire to contribute something new to the world, I wanted to be an inventor. The spirit of the NIAC program I believe perfectly correlates with my personal vision and it is actualizing to have NIAC also agree that the technology that I am working on is game changing.

Thank you to Paolo Venneri (USNC-Tech's CEO) who supported the EmberCore technology ever since I proposed the idea in 2019. There has been a lot of support at USNC-Tech and internal support and resources (including writing the Phase I proposal).

Thank you to my coworkers who helped provide expertise and feedback including Danyal Turkoglu, Tanek Ballachanda, Marta Soltyszevska, Cherie Austin, Brian Coulter, Jack Ackerman, Lorenzo Venneri, and Sara Pelka. It is a team effort, and all of you really moved the ball both on technical and administrative tasks. I also wanted to acknowledge many teachers, professors, and family who have left an indelible mark on my life, indirectly leading to this Phase I NIAC.

I wanted to acknowledge my wife Jacqueline Morrison who put up with my geeking out all the time and for the times I put in long hours. Your support is even more appreciated as we are expecting our first child in March.

*Christopher Morrison Ph.D.*

*Extrasolar Express NIAC Phase I Principal Investigator*

*Astro Nuclear Engineer, USNC-Tech*

*c.morrison@usnc-tech.com* olar Express NIAC Phase I Principal Investigator

*Astro Nuclear Engineer, USNC-Tech*

[c.morrison@usnc-tech.com](mailto:c.morrison@usnc-tech.com)

## 9. References

1. File:Interstellar visitors.jpg - Wikimedia Commons. Available at: <https://commons.wikimedia.org/w/index.php?curid=82114871>. (Accessed: 19th September 2019)
2. Ivezić Z. *et al.* LSST: From Science Drivers to Reference Design and Anticipated Data Products. *Astrophys. J.* **873**, 111 (2019).
3. Trilling, D. E. *et al.* Implications for Planetary System Formation from Interstellar Object 1I/2017 U1 ('Oumuamua). *Astrophys. J.* **850**, L38 (2017).
4. ESA Newsroom and Media Relations. ESA's New Mission to Intercept a Comet. 2019 Available at: <https://sci.esa.int/web/cosmic-vision/-/61416-esa-s-new-mission-to-intercept-a-comet>. (Accessed: 19th September 2019)
5. Gray, B. Pseudo-MPEC for A/2017 U1 = 1I = 'Oumuamua. *Project Pluto* Available at: <https://projectpluto.com/temp/2017u1.htm>. (Accessed: 19th September 2019)
6. Solar Power Technologies for Future Planetary Science, NASA, [https://solarsystem.nasa.gov/system/downloadable\\_items/715\\_Solar\\_Power\\_Tech\\_Report\\_FINAL.PDF](https://solarsystem.nasa.gov/system/downloadable_items/715_Solar_Power_Tech_Report_FINAL.PDF)
7. R. Bechtel, Multi-Mission Radioisotope Thermoelectric Systems, Department of Energy, [https://www.nasa.gov/sites/default/files/files/4\\_Mars\\_2020\\_MMRTG.pdf](https://www.nasa.gov/sites/default/files/files/4_Mars_2020_MMRTG.pdf)
8. C. Morrison, Temperature and Power Specific Mass Scaling for LEU Closed Cycle Brayton Systems for Space Surface Power and Nuclear Electric Propulsion <http://anstd.ans.org/NETS-2019-Papers/Track-6--Energy-Conversion-Technology-and-Development/abstract-126-0.pdf>
9. A. Davoyan "Extreme Solar Sailing for Breakthrough Space Exploration" NIAC [https://www.nasa.gov/directorates/spacetech/niac/2021\\_Phase\\_I/Extreme\\_Solar\\_Sailing\\_for\\_Breakthrough\\_Space\\_Exploration/](https://www.nasa.gov/directorates/spacetech/niac/2021_Phase_I/Extreme_Solar_Sailing_for_Breakthrough_Space_Exploration/)
11. "Interstellar object, named Oumuamua, likely a cookie-shaped planet shard, study reveals" ABC News <https://www.abc.net.au/news/2021-03-18/interstellar-object-is-cookie-shaped-planet-shard/100016164> (March 2021)
12. E. Gough "Cosmic rays erode away all but the largest interstellar objects" <https://phys.org/news/2021-09-cosmic-rays-erode-largest-interstellar.html> (Sept. 2021)
13. K. Hickok "Interstellar visitor 'Oumuamua wasn't a nitrogen iceberg, Harvard astrophysicists say" Life Science <https://www.livescience.com/oumuamua-not-nitrogen-iceberg> (Nov. 2021)
14. A. Hibberd, A. M. Hein, T. M. Eubanks, "Project Lyra: Catching 1I/'Oumuamua – Mission opportunities after 2024," *Acta Astronautica*, Vol. 170 pp. 136-144 (2020)
15. EmberCore Technology Homepace USNC <https://usnc.com/embercore/>
16. Dan Clayton
17. J. Casani, Space Fission Power: NASA's Bets Bet to Continue to Explore the Outer Solar System, NETS 2019, Richland, Washington, <http://anstd.ans.org/NETS-2019-Papers/Track-2--Mission-Concepts-and-Logistics/abstract-127-0.pdf>
18. H. Yano "The Hayabusa Asteroid Sample Return Mission,"

- <https://www.lpi.usra.edu/meetings/am2005/pdf/7030.pdf>
19. C. Lisse et. al. Deep Impact and Sample Return, *Journal of Earth Planets and Space*, **60** 61-66, 2008, <https://link.springer.com/content/pdf/10.1186%2F03352762.pdf>
  20. Hofer, R. R., Cusson, S. E., Lobbia, R. B. & Gallimore, A. D. The H9 Magnetically Shielded Hall Thruster. *35th Int. Electr. Propuls. Conf. IEPC-2017-232* (2017).
  21. Dudenhoefer, J. E. & Winter, J. M. Status of NASA's Stirling Space Power Converter Program. *Proc. Intersoc. Energy Convers. Eng. Conf.* **2**, 38–43 (1991).
  22. Foster, J. et al. The High Power Electric Propulsion (HiPEP) Ion Thruster. (2004). doi:10.2514/6.2004-3812
  23. Christopher G. Morrison (2020) Temperature and Power Specific Mass Scaling for Commercial Closed-Cycle Brayton Systems in Space Surface Power and Nuclear Electric Propulsion Applications, *Nuclear Technology*, 206:8, 1224-1239, DOI: [10.1080/00295450.2020.1738173](https://doi.org/10.1080/00295450.2020.1738173)
  24. Presidential Memorandum on Launch of Spacecraft Containing Space Nuclear Systems <https://trumpwhitehouse.archives.gov/presidential-actions/presidential-memorandum-launch-spacecraft-containing-space-nuclear-systems/>
  25. FEEP Thruster Product Page "<https://www.enpulsion.com/order>